

Carbon Deposition by Film Delamination and X-ray Mirror Curvature Control

Associate Professor Alex A. Volinsky, Ph.D.

Department of Mechanical Engineering

University of South Florida, Tampa, FL 33620

volinsky@eng.usf.edu

www.eng.usf.edu/~volinsky

July 21, 2011, INFN

Acknowledgements

Funding: National Science Foundation

NSF International Research Experience for Students (IRES) Program

People:

USF: Mykola Kurta, Michael Weinbaum, Evgeny Shakurov, Grygoriy Kravchenko,
Megan Pendergast, Ramakrishna Gunda, James Rachwal, Robert Shields,
Nathaniel Waldstein,

Prof. Nathan Crane, Prof. Craig Lusk

TU Dresden: Dirk Meyer, Alexandr Levin, Tillman Leisegang, Hartmut Stöcker,
Emanuel Gutmann, Dirk Spitzner, Torsten Weißbach, Irina Shakhverdova

DESY: Dmitri Novikov

X-FEL: Harald Sinn, Germano Galasso, Liubov Samoylova, Fan Yang, Antje Trapp

INFN: Roberto Cimino, David Grosso, Roberto Flammini, Rosanna Larciprete

Current IRES \$150K (with overhead)

3-4 summers, 4-5 students per summer (\$2,000/months + airline ticket)

Started in 2010. Grant supports travel and allowance

What Mechanical Engineering students skills are helpful?

- CAD/Design
- Data acquisition
- Mechanics of Materials
- FEM
- Thermodynamics/Heat transfer
- Fluid Mechanics
- Vibrations
- Robotics

Outline

- X-ray optics stability and control, temperature and strain distribution simulations
- Stress relief effects in thin films and multilayers
- Electrowetting experiments

Thin film residual stress

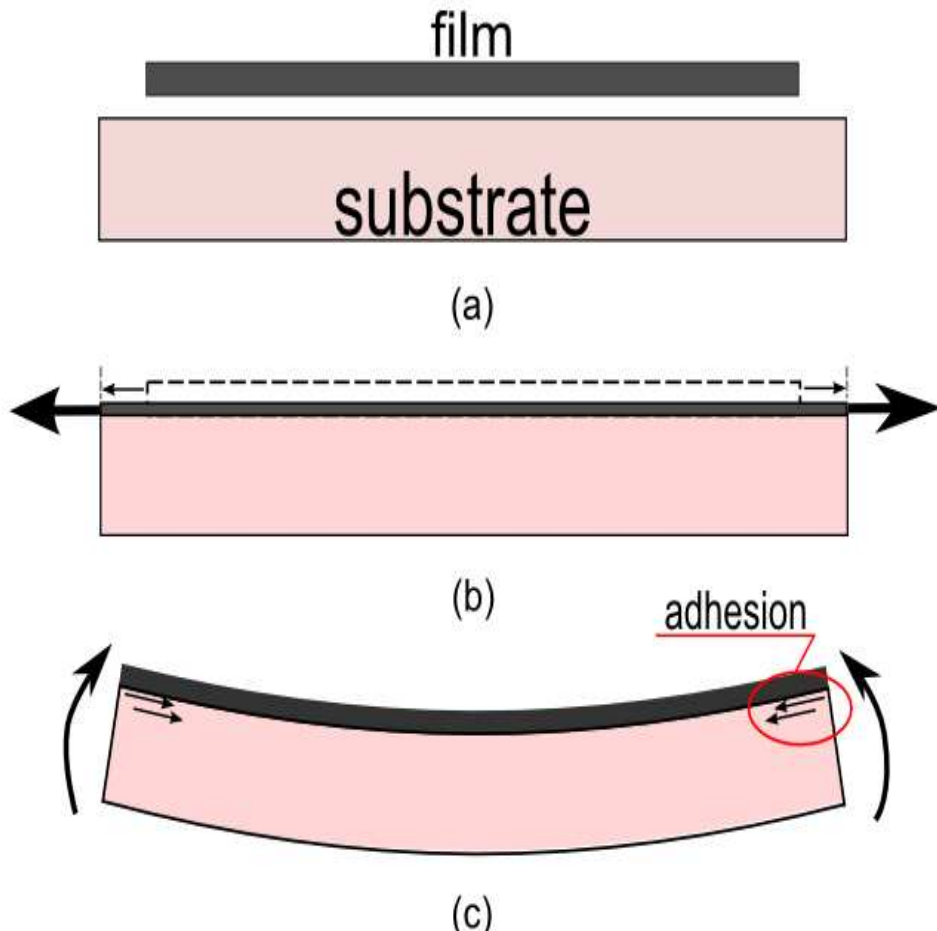
- Thermal } Total
- Intrinsic } residual
- Epitaxial } stress

Consequences

- New equilibrium state
- Failure
- Promotes diffusion

Length scales of stress

- Microscopic
- Macroscopic



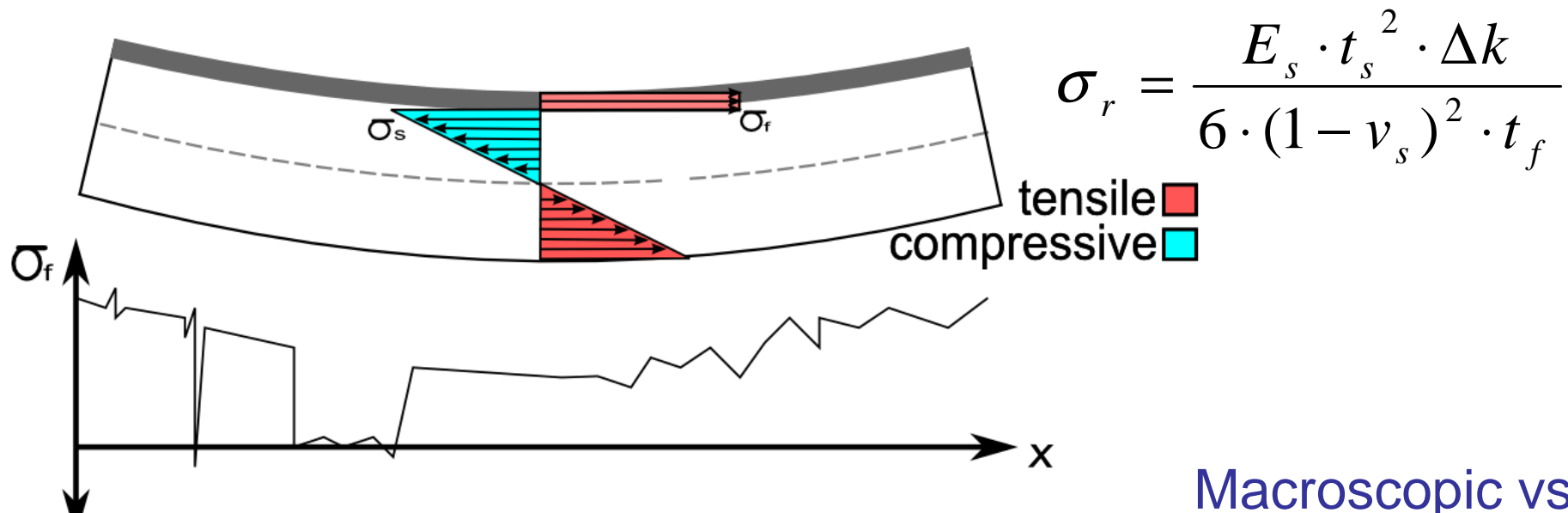
Measuring residual stress

Film material strain

- X-ray Diffraction
 - Bragg's law
- Raman spectroscopy

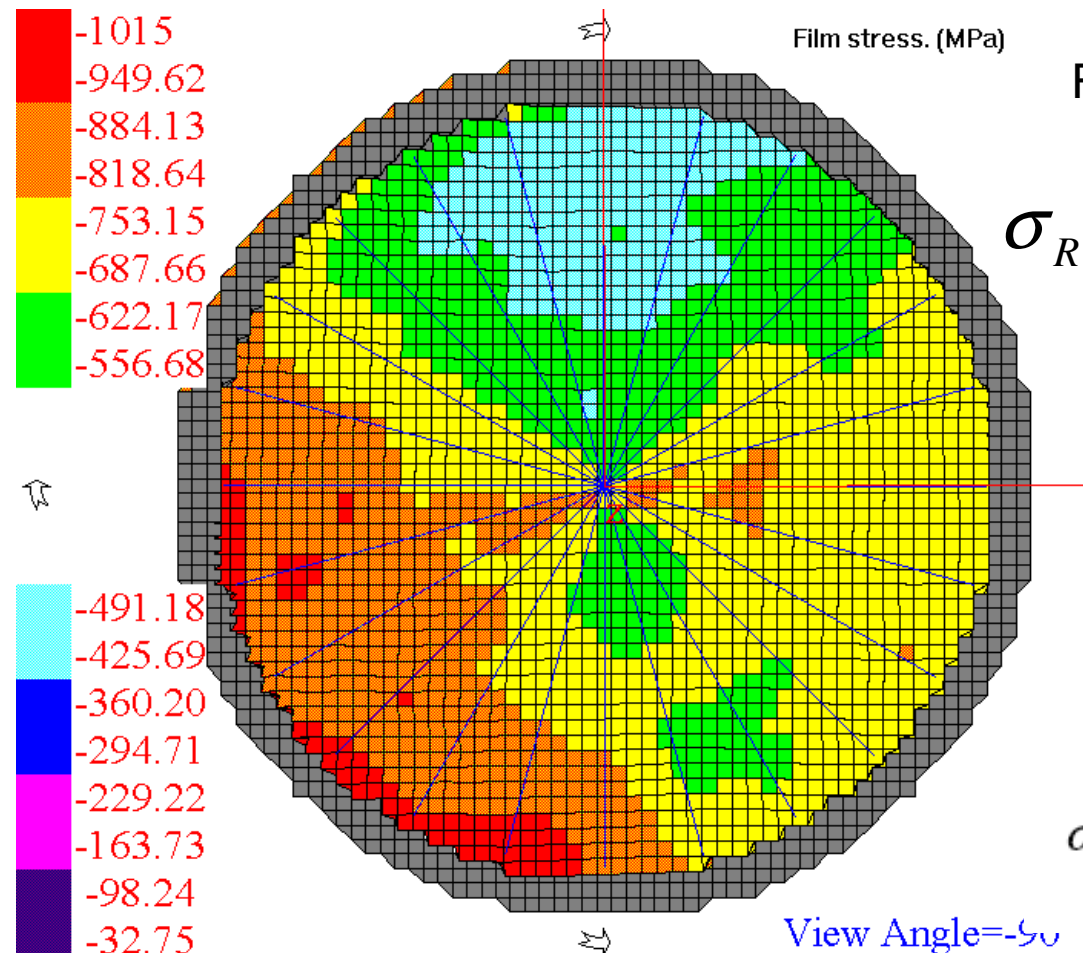
Substrate curvature

- Optical interferometry
- Optical profiling
- Mechanical profiling



Macroscopic vs.
Microscopic measurements

Modified Stoney Formulas



For non-uniform film thickness

$$\sigma_R(r) = \frac{E_s}{1-\nu_s} \frac{\Delta k(r) h_s^2}{6h_f(r)} c(r)$$

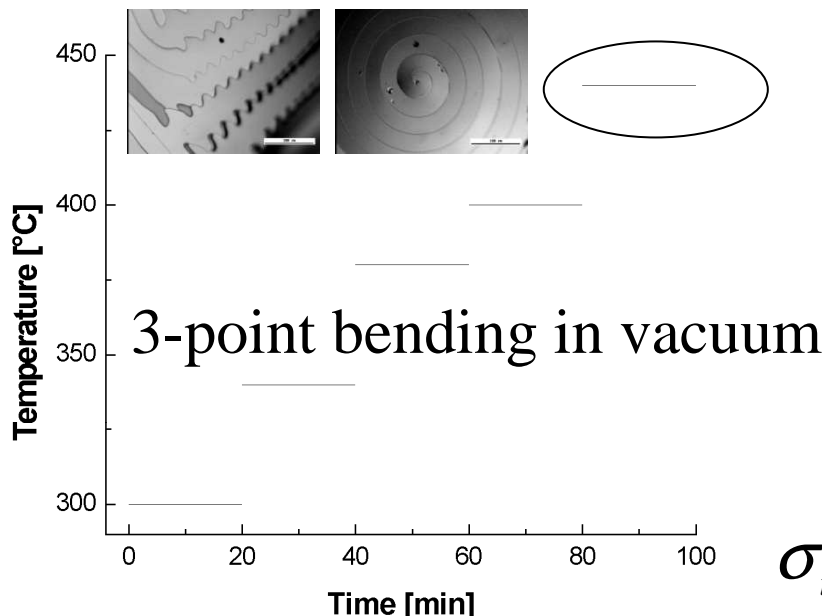
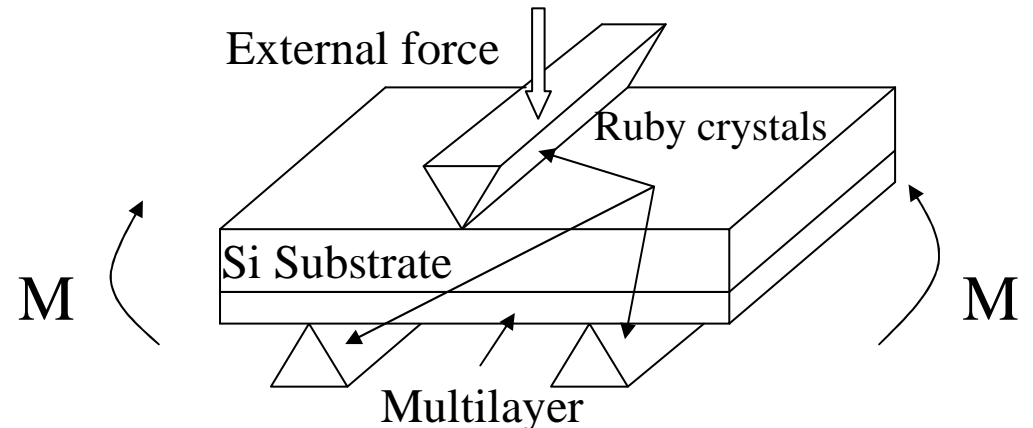
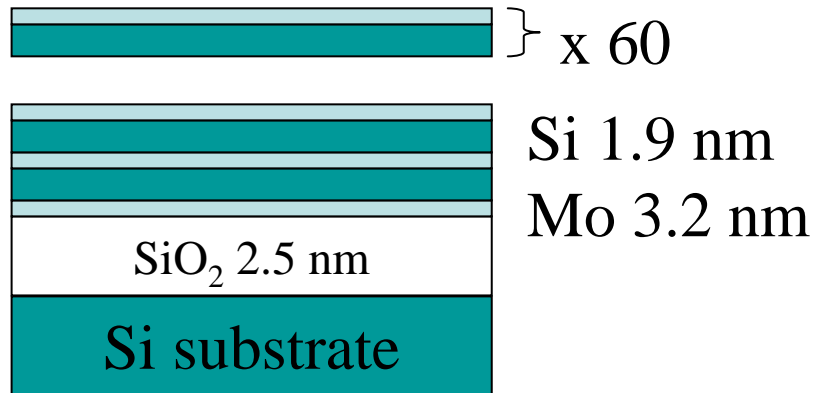
Residual Stress in CVD-grown 3C-SiC Films on Si Substrates, A.A. Volinsky, G. Kravchenko, P. Waters, J. Deva Reddy, C. Locke, C. Frewin, S.E. Saddow, Mat. Res. Soc. Symp. Proc. Vol. 1069, D3.5, 2008

2D case:

$$\sigma_R = \frac{E_s}{1-\nu_s} \frac{h_s^2}{6h_f R_1} \cdot \left[1 + \left[\frac{\nu}{1+\nu} \right] \cdot \left[\frac{R_1}{R_2} - 1 \right] \right]$$

TiWN film on 6" Si wafer

Mo/Si Mirror Bending Experiments



$$\sigma_r^{comp.} \approx 100 \text{ MPa}$$

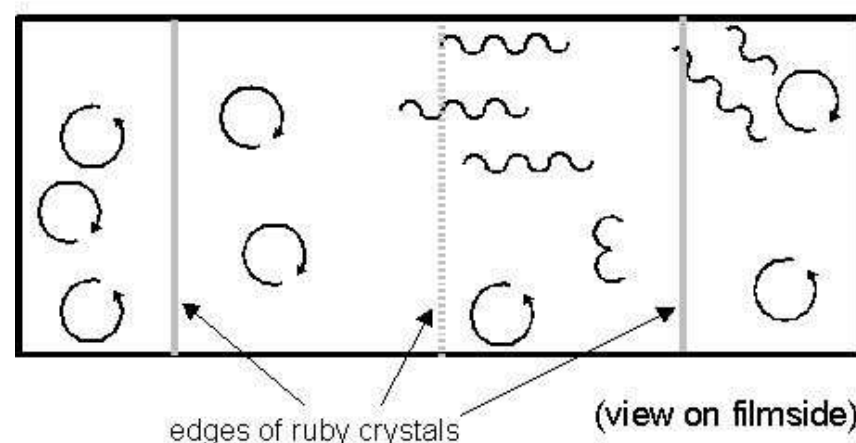
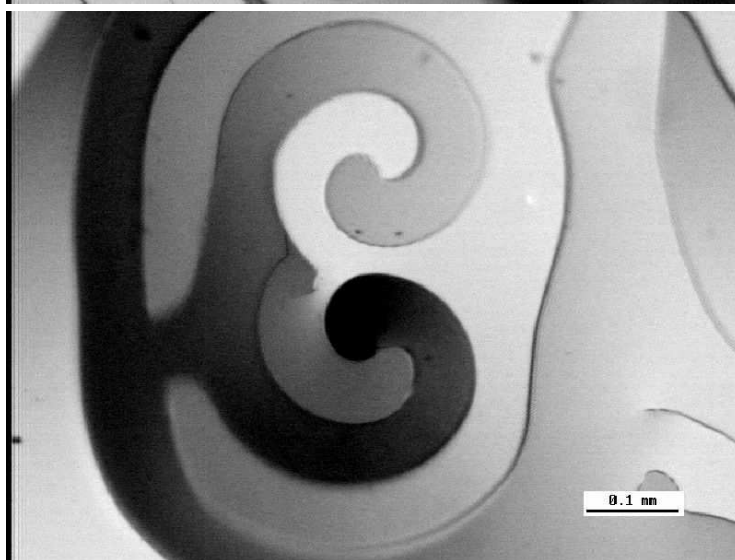
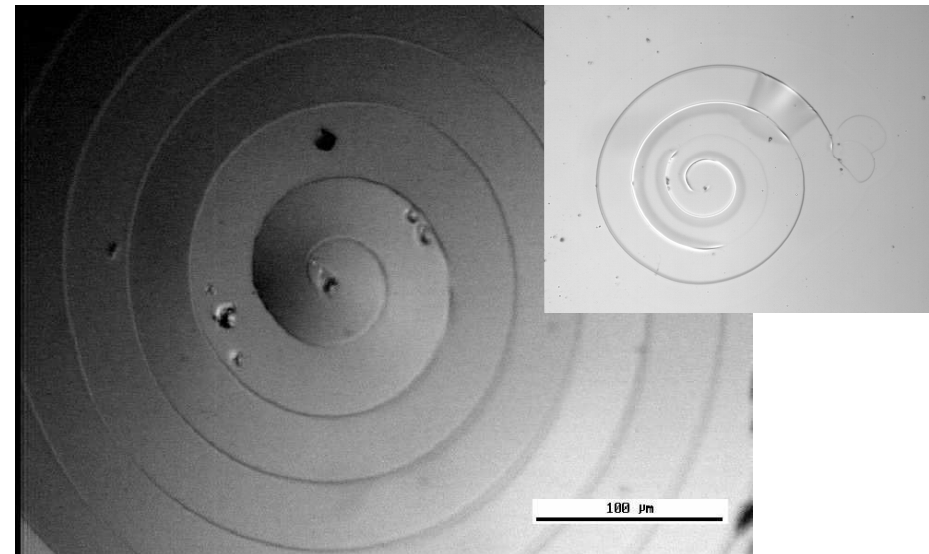
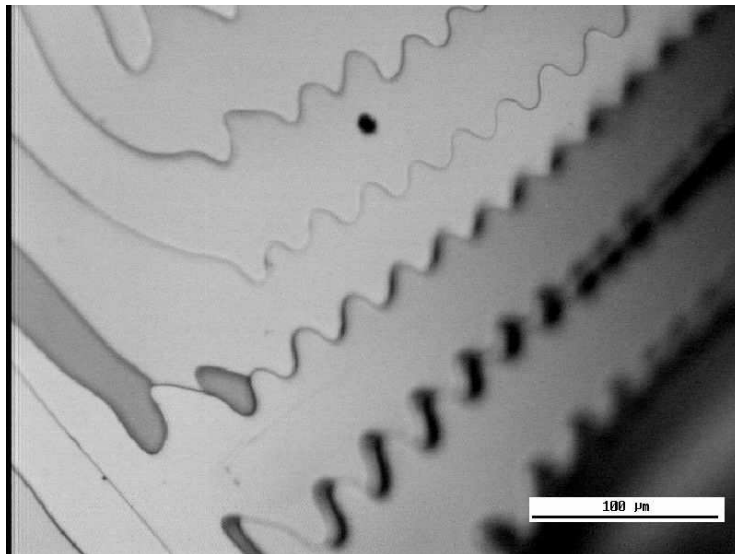
$$\sigma_T^{comp.} = \frac{\Delta\alpha \Delta TE_f}{1 - \nu_f} = 460 \text{ MPa}$$

$$\sigma_{bend}^{tens.} = \frac{Mt}{2I} = 225 \text{ MPa}$$

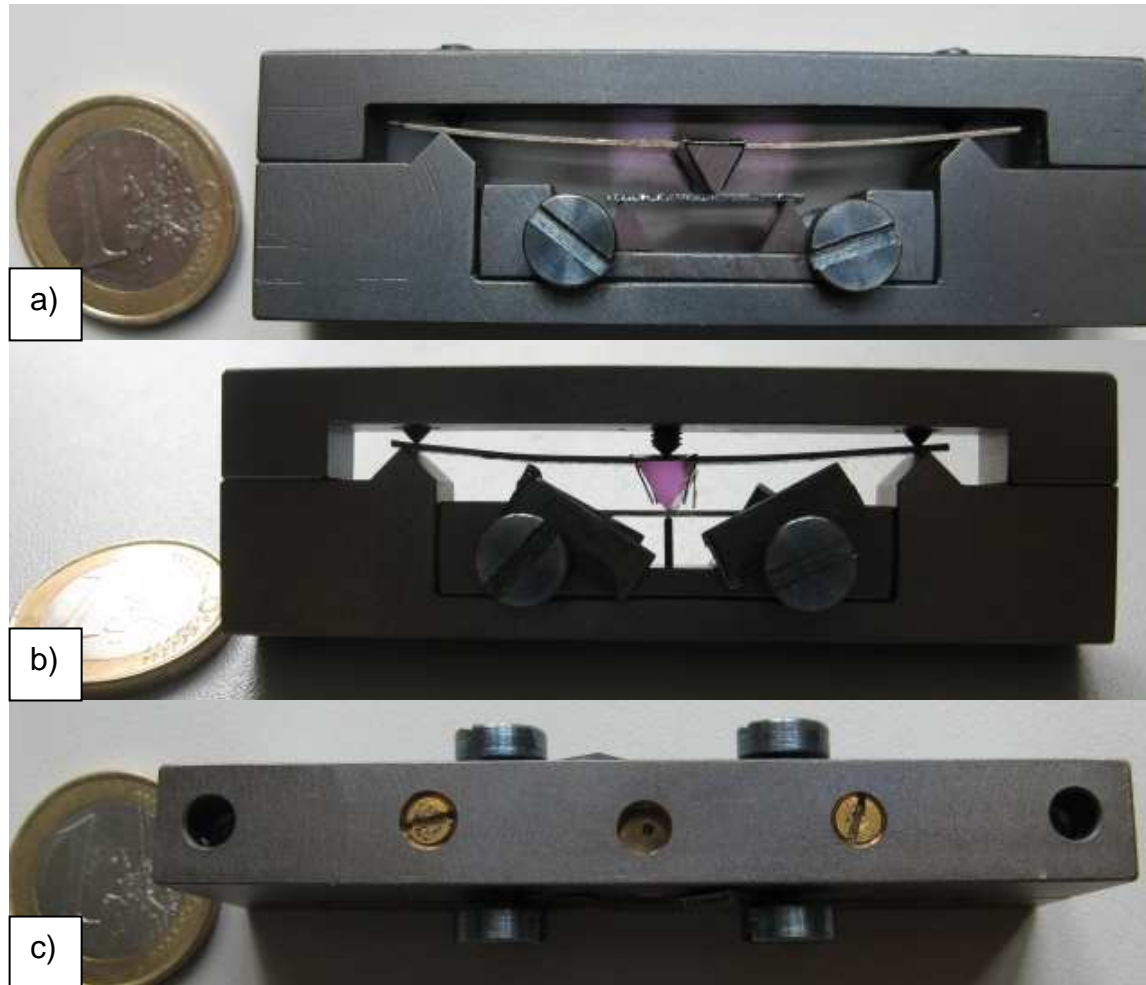
$$\sigma_{total}^{comp.} = \sigma_{residual} + \sigma_{bending} + \sigma_T = 335 \text{ MPa}$$

D.C. Meyer, T. Leisegang, A.A. Levin, P. Paufler, A.A. Volinsky, Appl. Phys. A 78, pp. 303-305, 2004

Tensile Crack Patterns: Mo/Si



3-point Bending Fixture Improvement

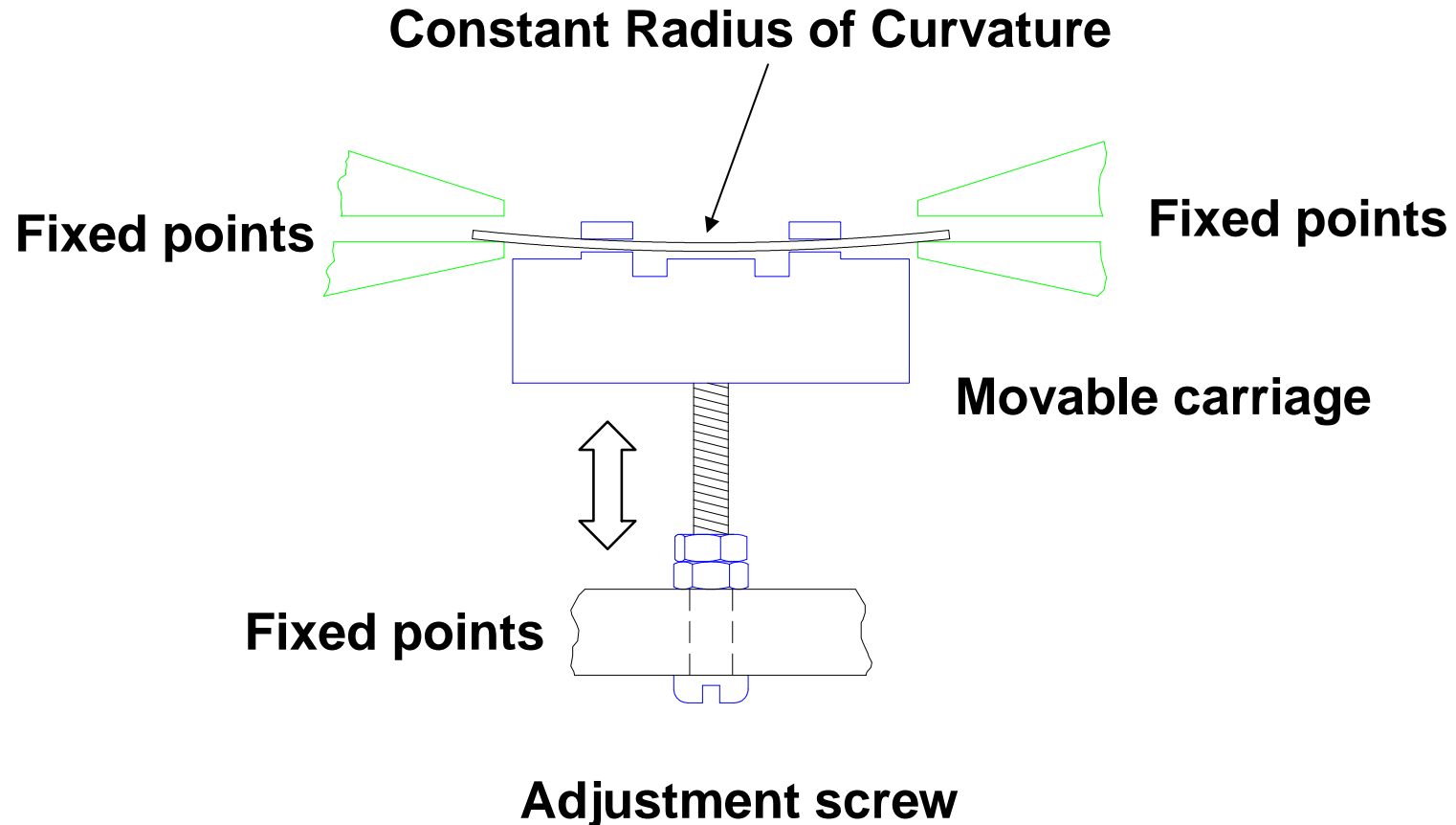


Before modification

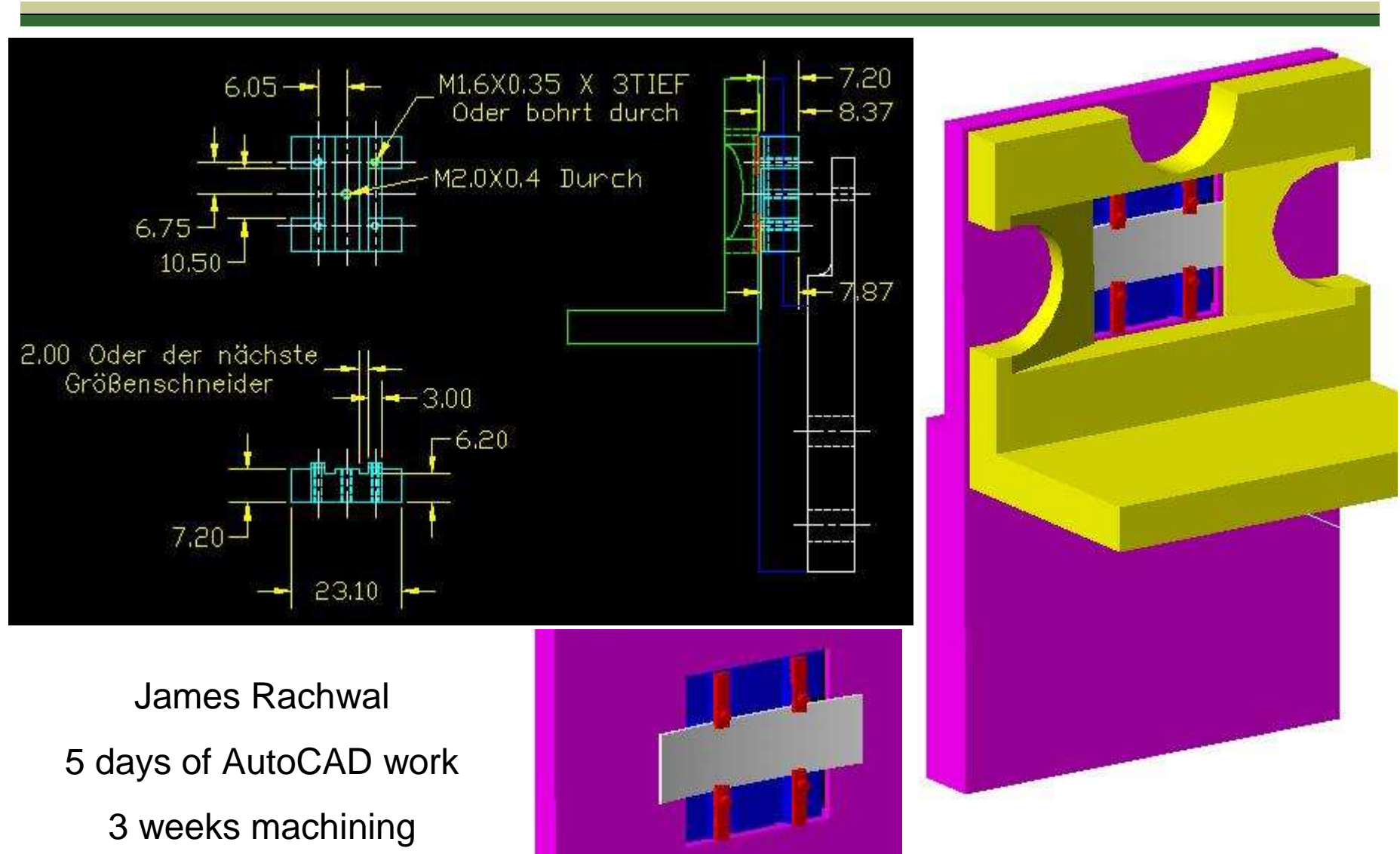
Modified fixture

80-100 μm beam
displacement,
15-19 N Force,
250-350 MPa max. normal
stress due to bending

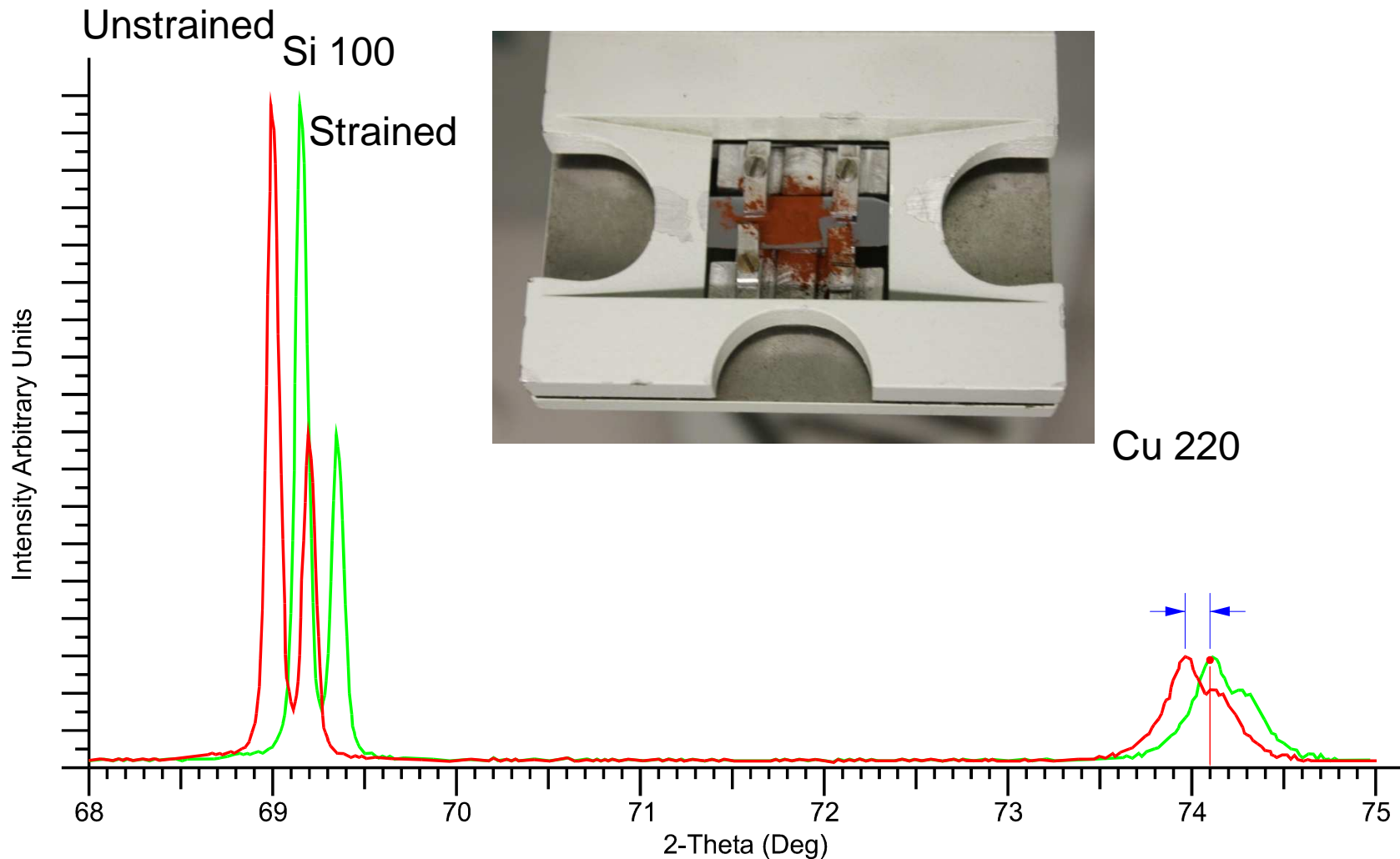
4-Point Bending Fixture



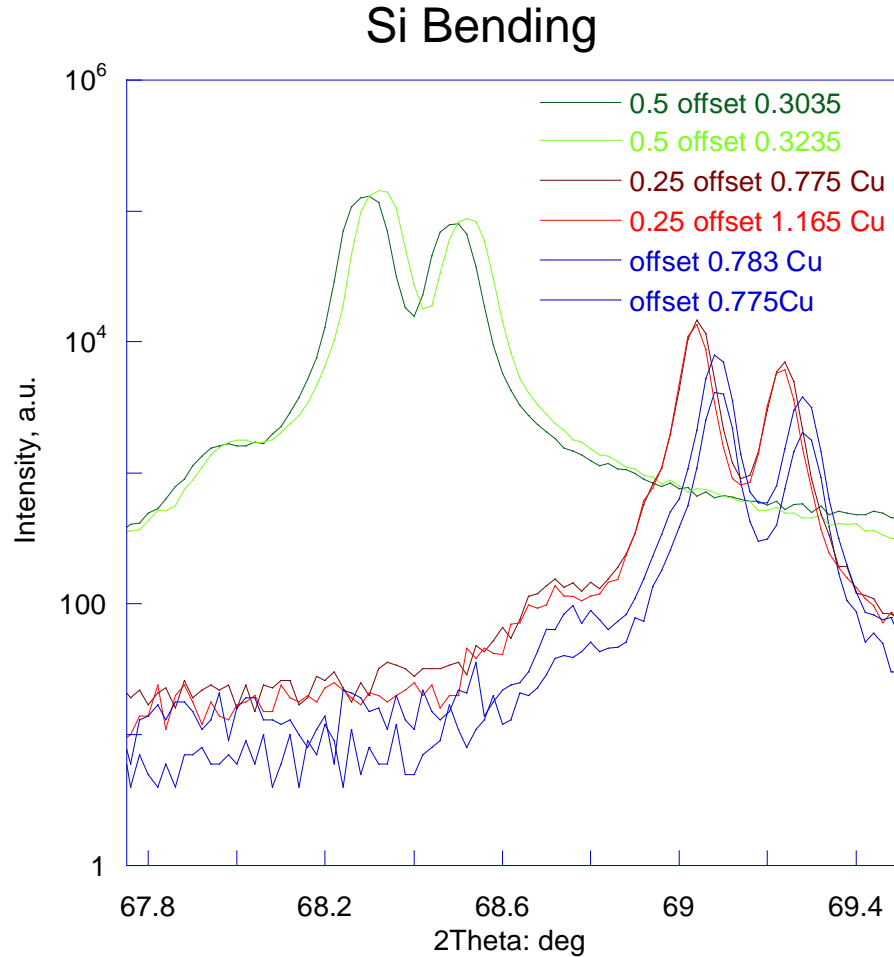
In-Situ 4-point Bending Fixture. Tension-Compression



Copper Powder Corrections

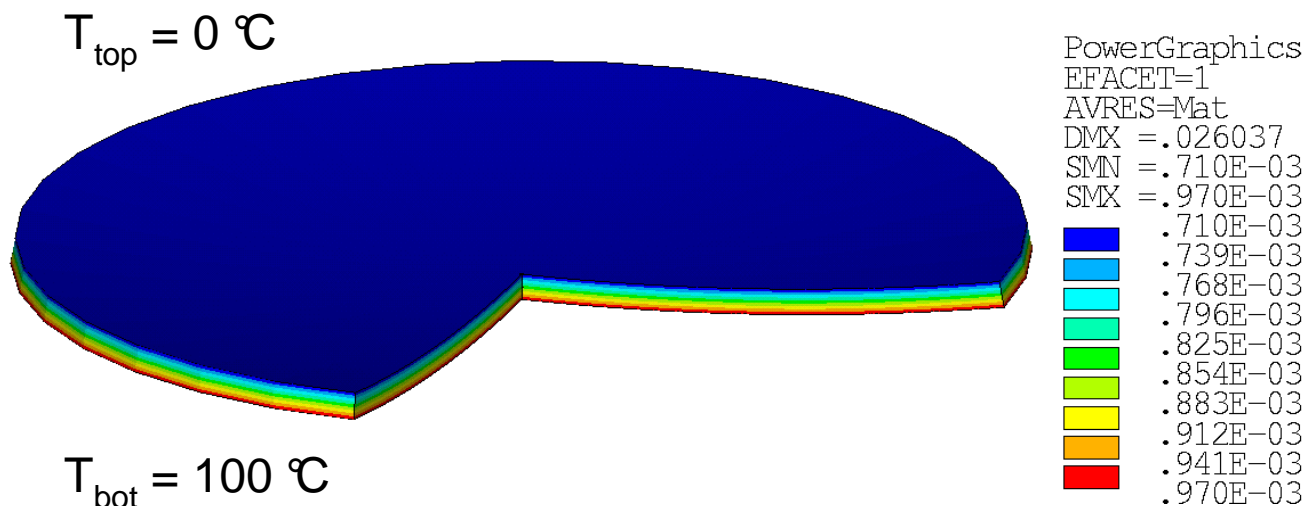


Bending Fixture Preliminary Data



Curvature due to temperature gradient T_z

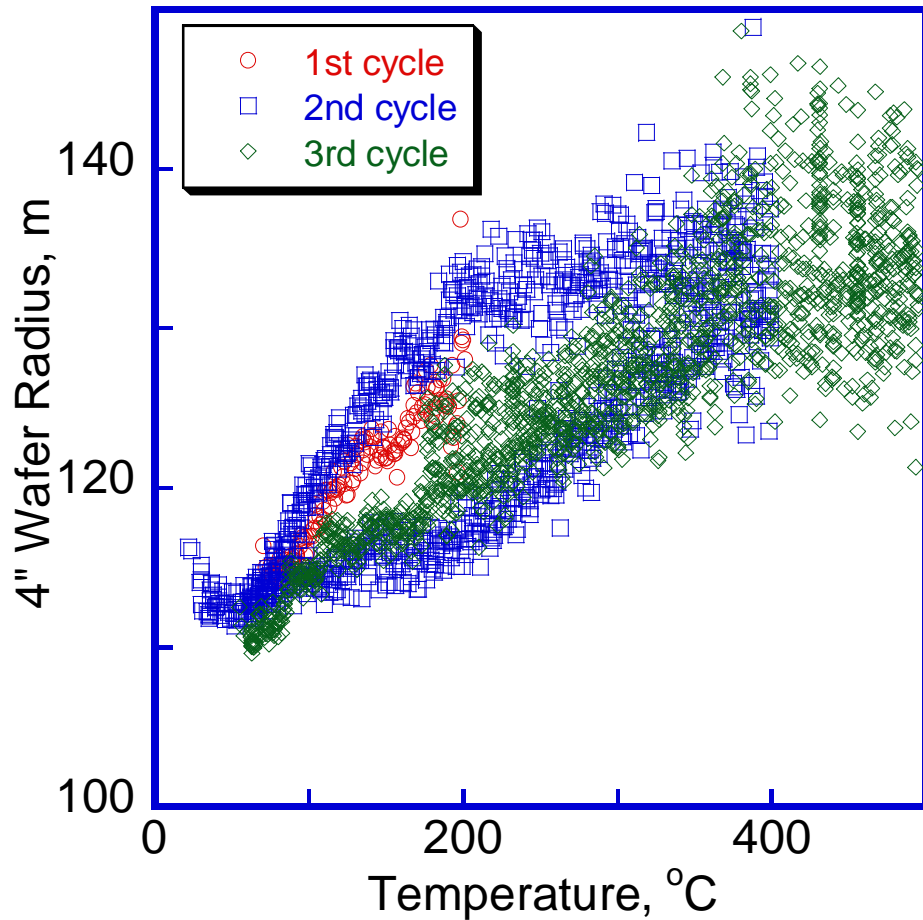
- Axisymmetric model of 0.5 mm Si substrate
- Steady-state
- No films, bare Si



- Radius of curvature: $R = 2 \text{ m}$

Grygoriy Kravchenko
Modeling GIGO problem

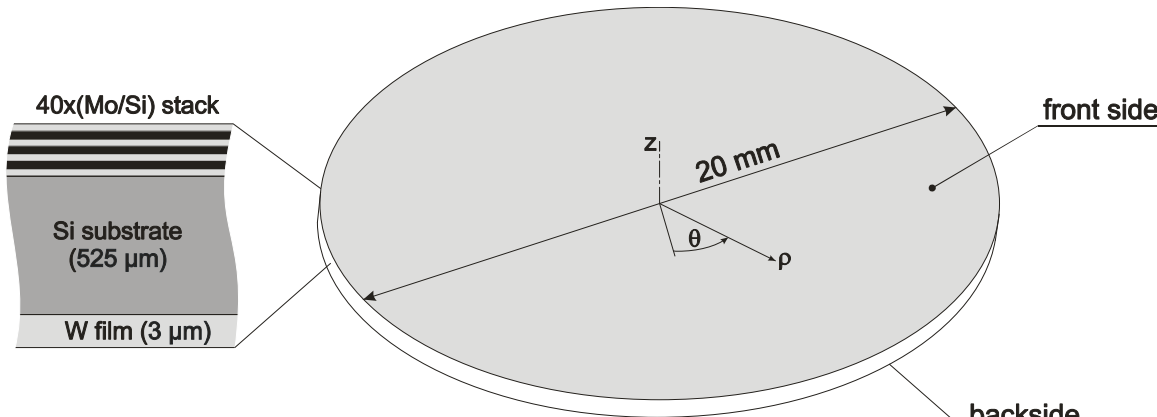
4" Si Wafer Uniform Heating



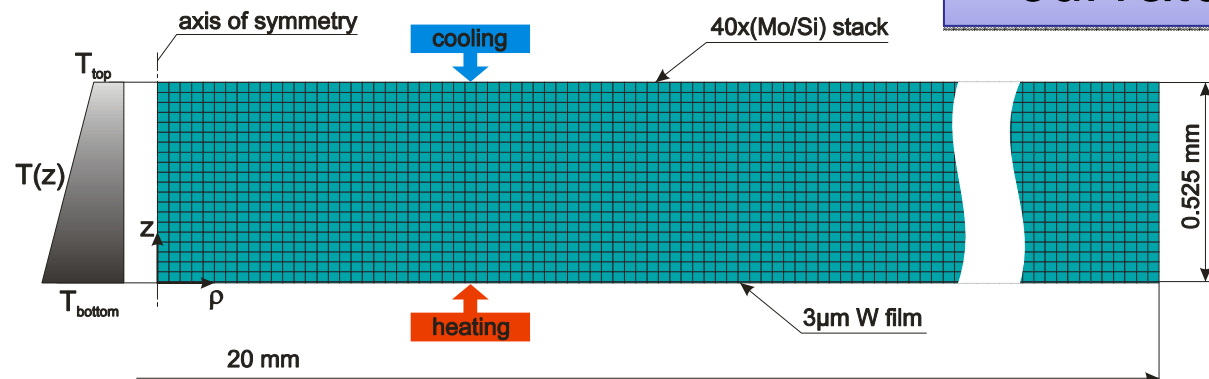
Uniform slow heating, wafer becomes flatter with T due to thin SiO_2 layer,

Similar to the simulation results

Temperature gradient with films



- Target radius of curvature:
 $R = 10 \text{ m}$
- $T_{\text{upper}} = 100 \text{ }^{\circ}\text{C}$

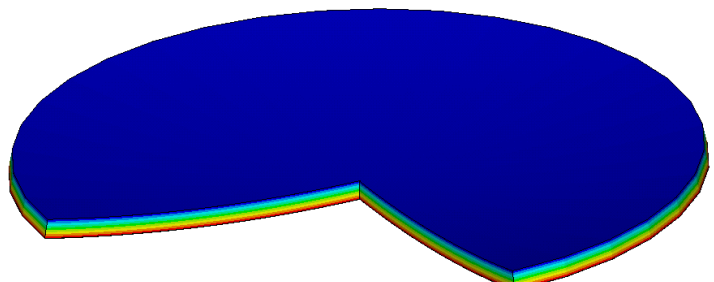


Thermally-induced
curvature control?

Axisymmetric finite element model

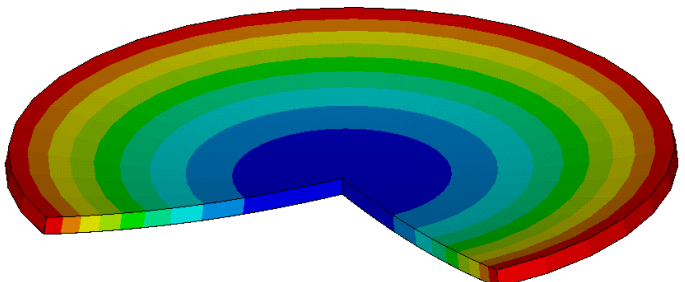
Temperature gradient $\Delta T_z = 20 \text{ } ^\circ\text{C}$

Total radial strains

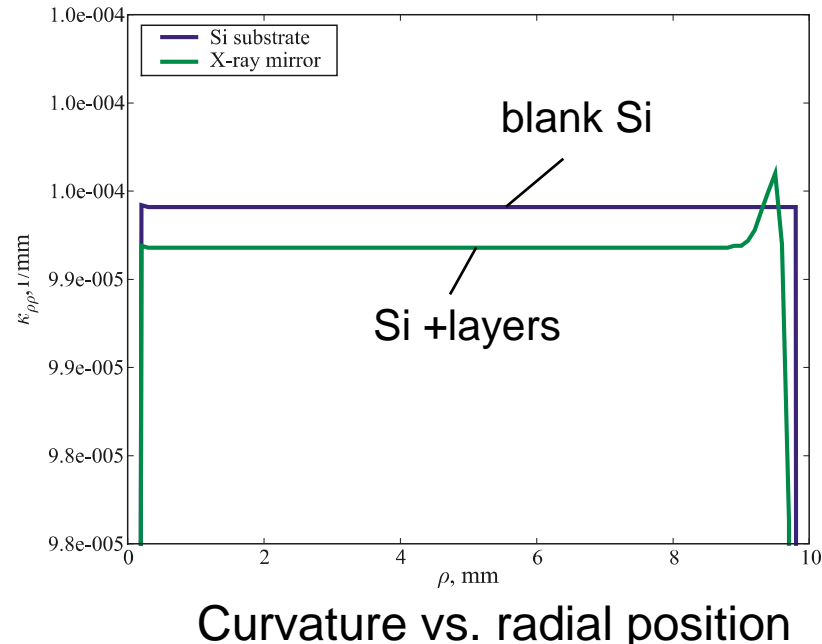


```
NODAL SOLUTION  
STEP=1  
SUB =1  
TIME=1  
/EXPANDED  
EPTIX (AVG)  
RSYS=0  
PowerGraphics  
EFACET=1  
AVRES=Mat  
DMX =.004224  
SMN =-.101E-05  
SMX =.517E-04  
-.101E-05  
.485E-05  
.107E-04  
.166E-04  
.224E-04  
.283E-04  
.341E-04  
.400E-04  
.458E-04  
.517E-04
```

Out-of-plane displacement



```
NODAL SOLUTION  
STEP=1  
SUB =1  
TIME=1  
/EXPANDED  
UY (AVG)  
RSYS=0  
PowerGraphics  
EFACET=1  
AVRES=Mat  
DMX =.004999  
SMN =-.131E-04  
SMX =.004984  
-.131E-04  
.542E-03  
.001097  
.001653  
.002208  
.002763  
.003318  
.003874  
.004429  
.004984
```



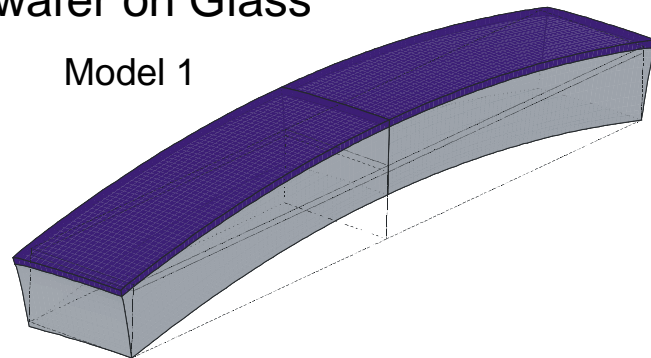
Curvature vs. radial position

- Curvature is uniform - spherical surface (small deformations)
- Influence of Mo/Si and W layers is small (thermal mismatch is negligible)

X-ray mirror deformed shape

Si wafer on Glass

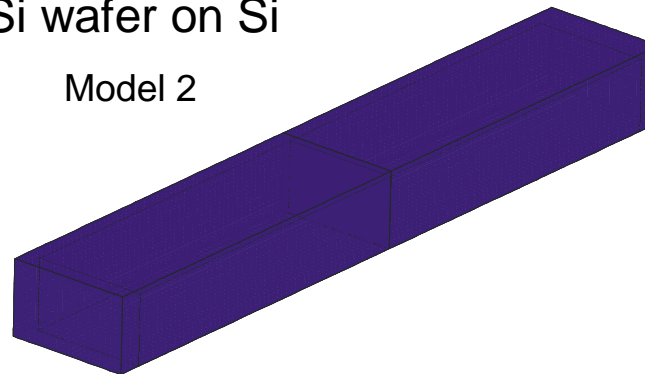
Model 1



largest thermal expansion mismatch

Si wafer on Si

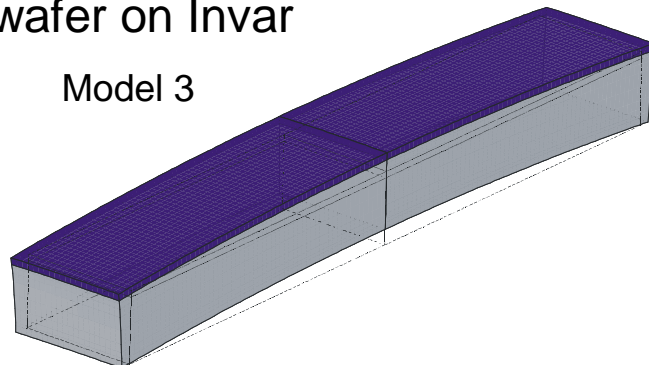
Model 2



no thermal expansion mismatch

Si wafer on Invar

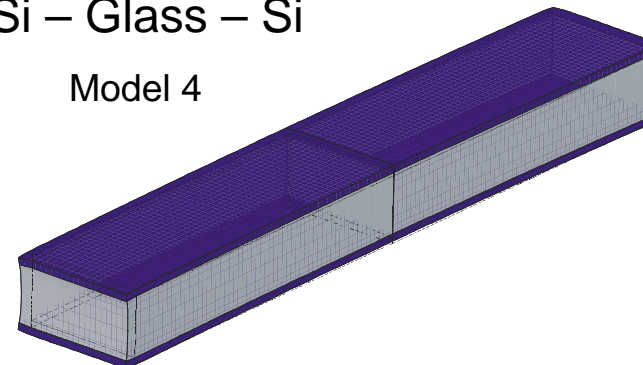
Model 3



smallest thermal expansion mismatch

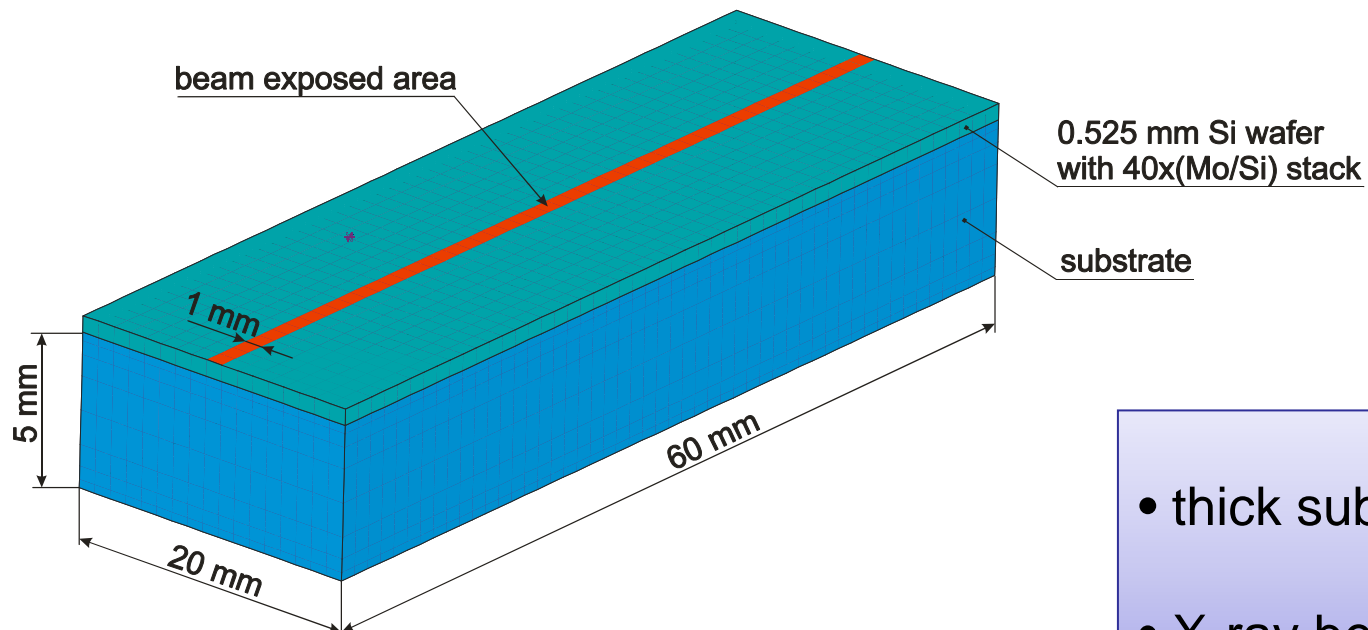
Si – Glass – Si

Model 4



compensated thermal expansion mismatch

X-ray mirror thermal deformations



- thick substrate
- X-ray beam: 1 W/cm²

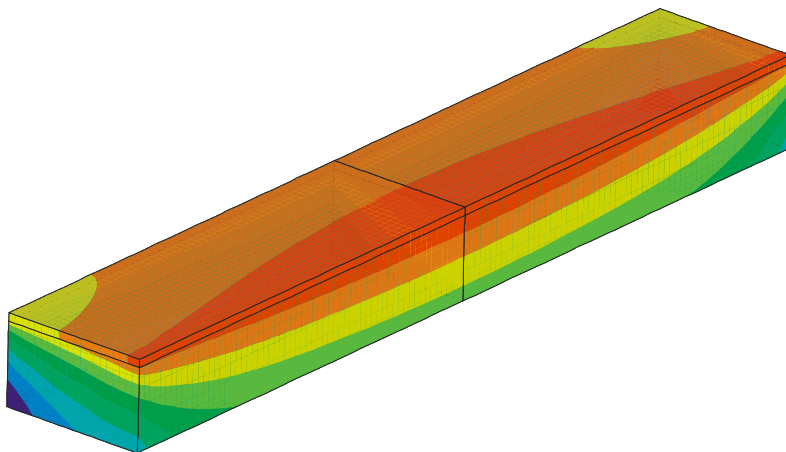
1. Solve the thermal problem
2. Solve the structural problem

Identify materials/geometry influence

Model variations:

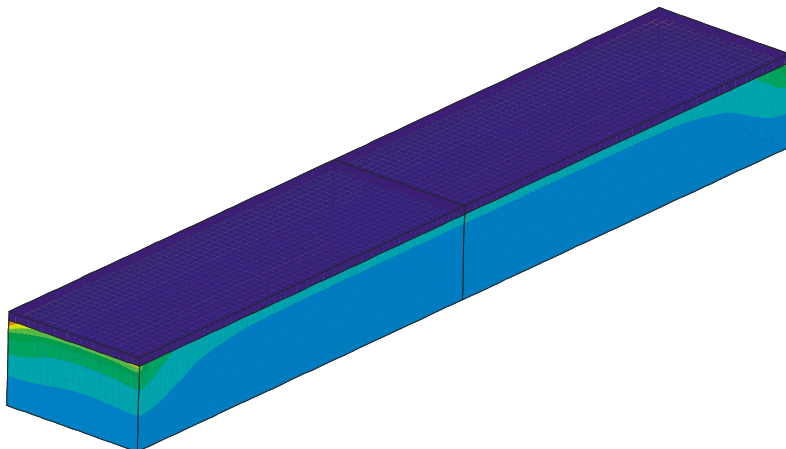
1. Si wafer on Glass
2. Si wafer on Si
3. Si wafer on Invar
4. Si wafer – Glass – Si wafer

Thermal results (Model 1)



```
PLOT NO. 1  
NODAL SOLUTION  
STEP=1  
SUB =1  
TIME=125  
/EXPANDED  
TEMP (AV)  
RSYS=0  
PowerGraphic  
EFACET=1  
AVRES=Mat  
SMN =312.244  
SMX =314.574  
312.244  
312.503  
312.762  
313.021  
313.28  
313.538  
313.797  
314.056  
314.315  
314.574
```

- temperature increases up to 15 °C
- almost uniform temperature distribution

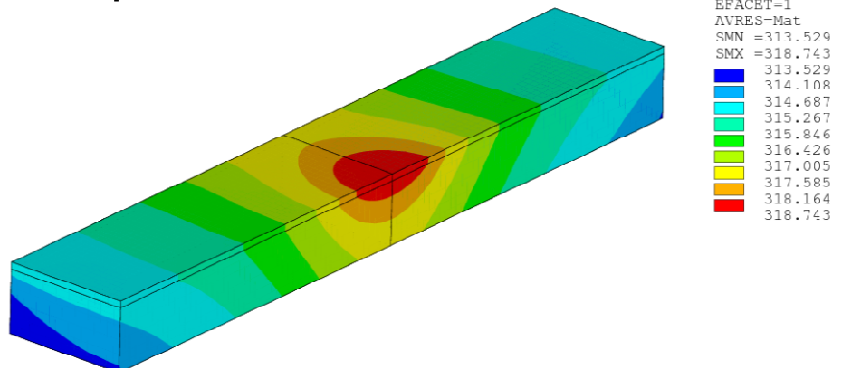


```
PLOT NO. 1  
NODAL SOLUTION  
STEP=1  
SUB =1  
TIME=125  
/EXPANDED  
TGZ (AV)  
RSYS=0  
PowerGraphic:  
EFACET=1  
AVRES=Mat  
SMN =-1.408  
SMX =935.656  
-1.408  
102.71  
206.829  
310.947  
415.065  
519.183  
623.301  
727.42  
831.538  
935.656
```

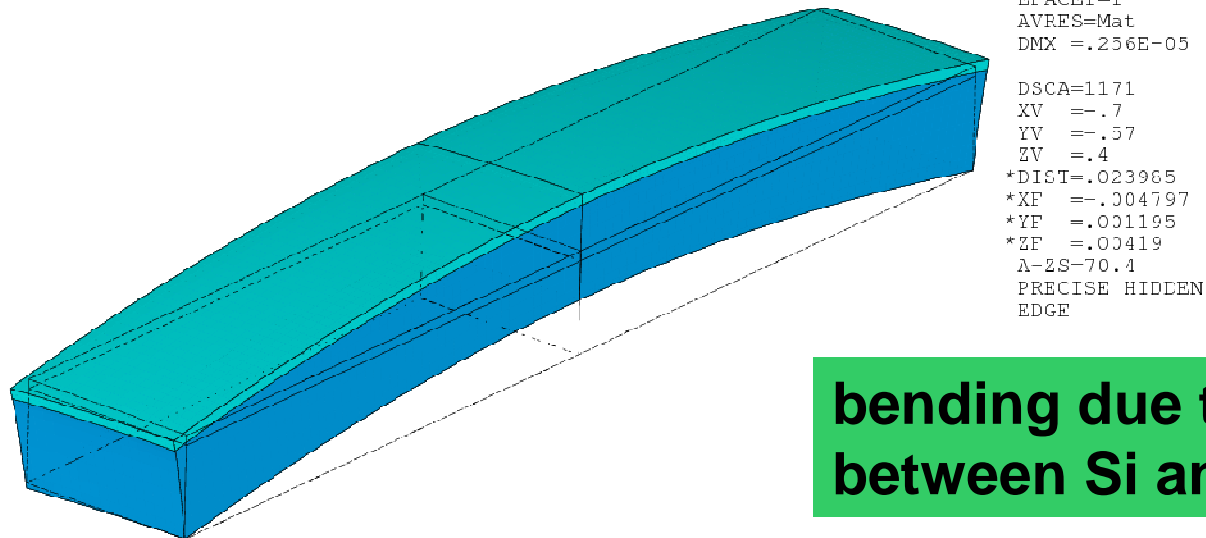
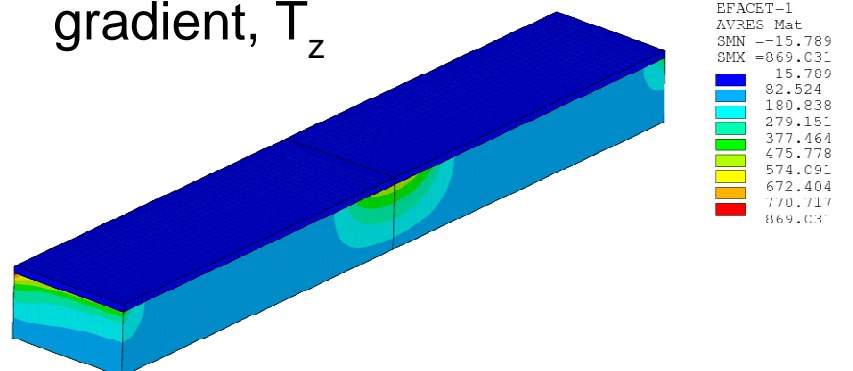
- very small temp. gradient ∇T_z in Si
- small ∇T_z in glass (<0.1 °C/mm) (away from the material corners)

Si on Glass substrate, 1 W/cm²

temperature field

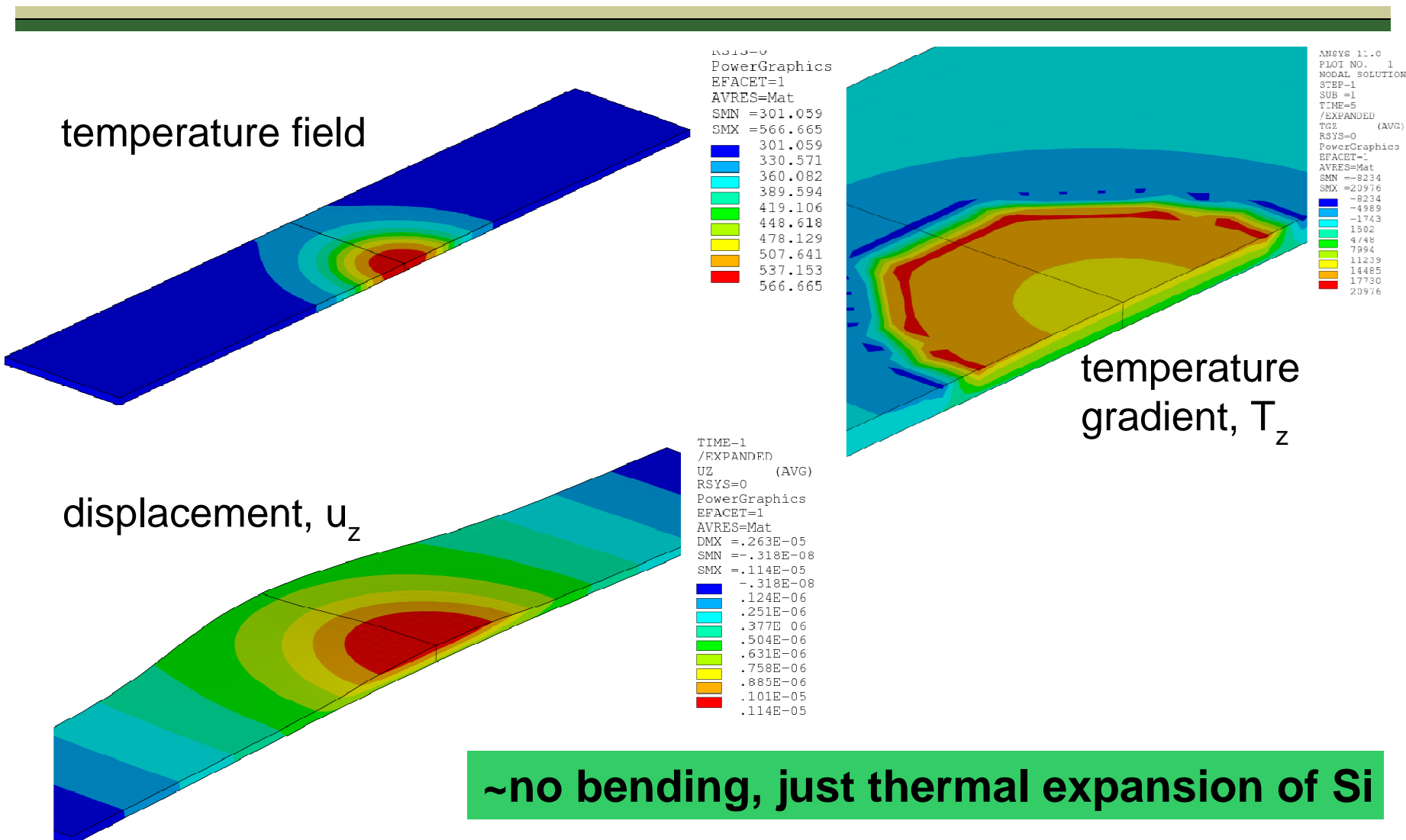


temperature gradient, T_z

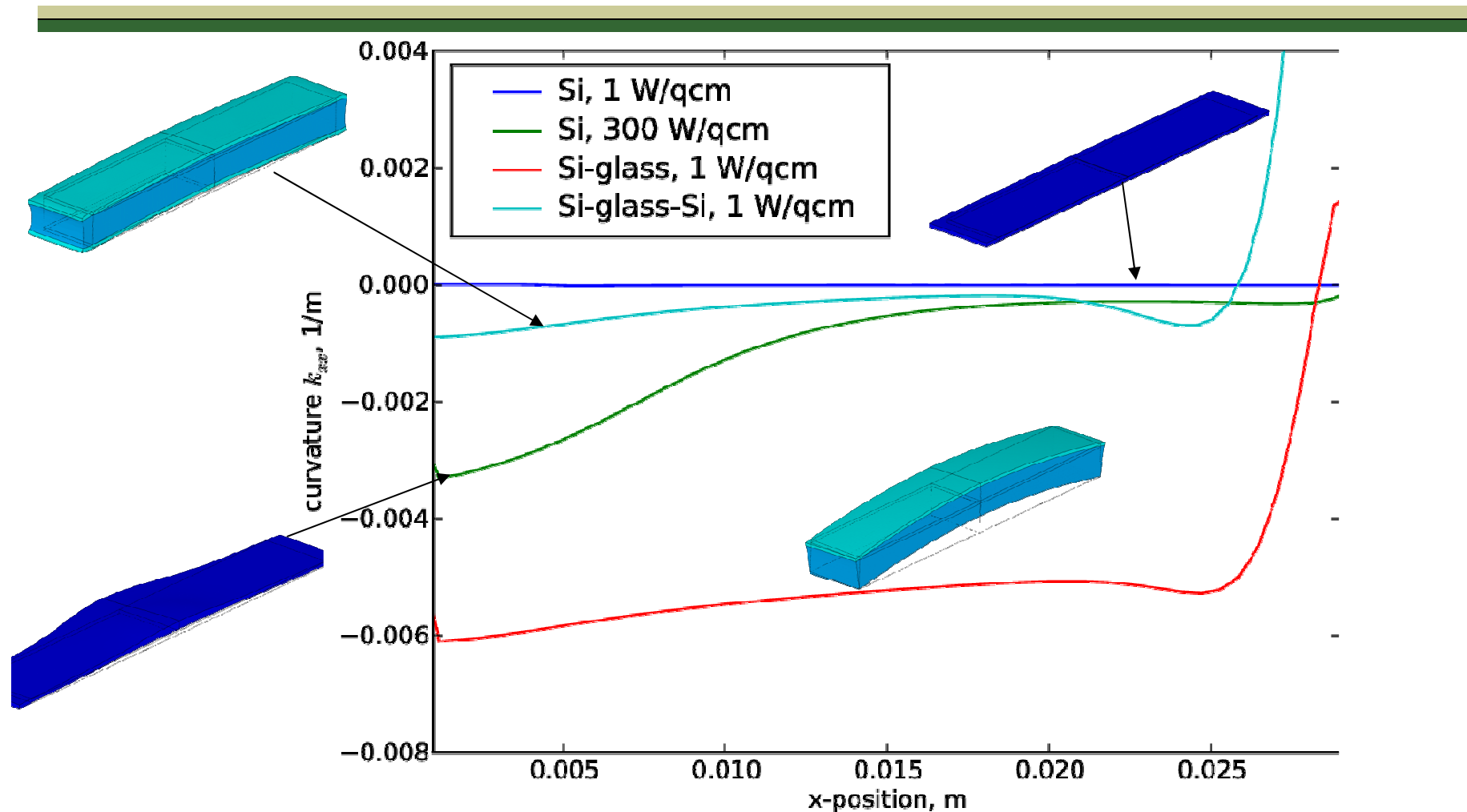


bending due to Δ CTE
between Si and glass substrate

Si, 300 W/cm² (BESSY)



Curvature



highest curvature with Si on Glass

FEM: X-ray mirror thermal deformations

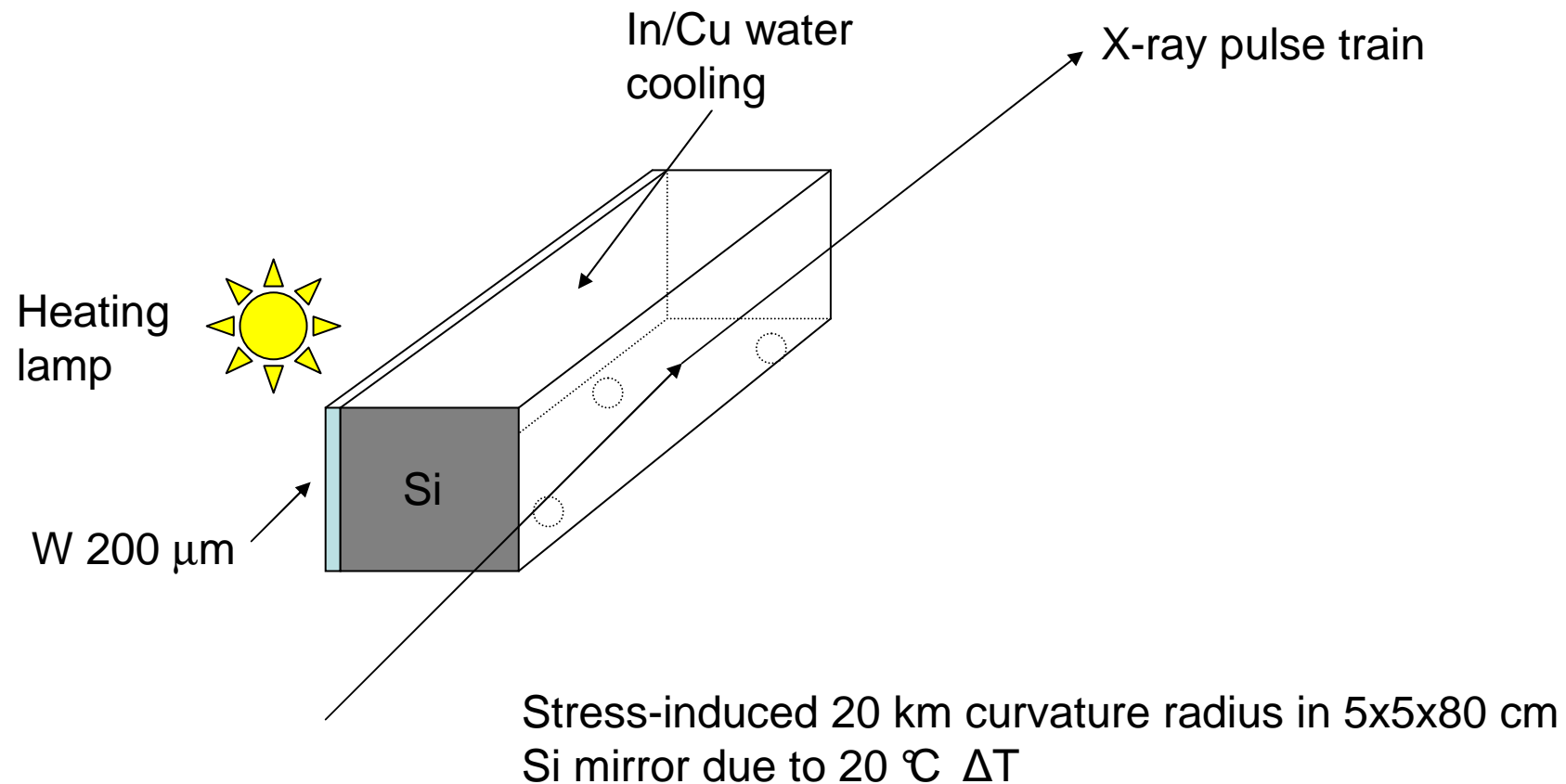
1. X-ray mirror (Si wafer):

- a) Target radius of curvature $R = 10 \text{ m}$ can be achieved by application of the through-thickness temperature gradient of about $20 \text{ }^{\circ}\text{C}$
- b) the upper limit ($RT+20 \text{ }^{\circ}\text{C}$) does not exceed the maximum operational temperature of $100 \text{ }^{\circ}\text{C}$

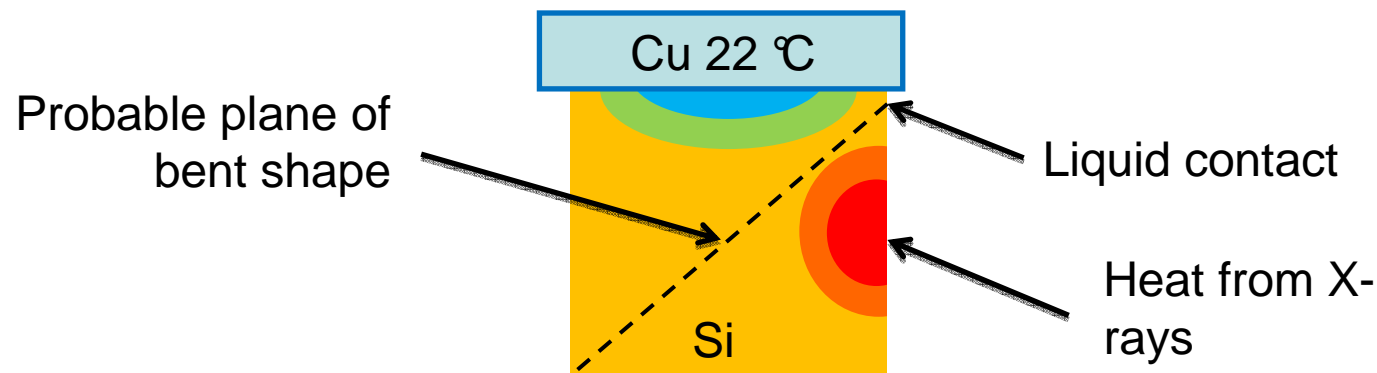
2. Optics element exposed to the X-ray beam:

- a) temperature distribution is almost uniform (in steady-state)
- b) X-ray beam with the power of 1 W/cm^2 heats the structure up to $15 \text{ }^{\circ}\text{C}$
- c) minimization or compensation of the thermal expansion mismatch is an effective way to reduce thermal deformations

XFEL Mirror Curvature Control

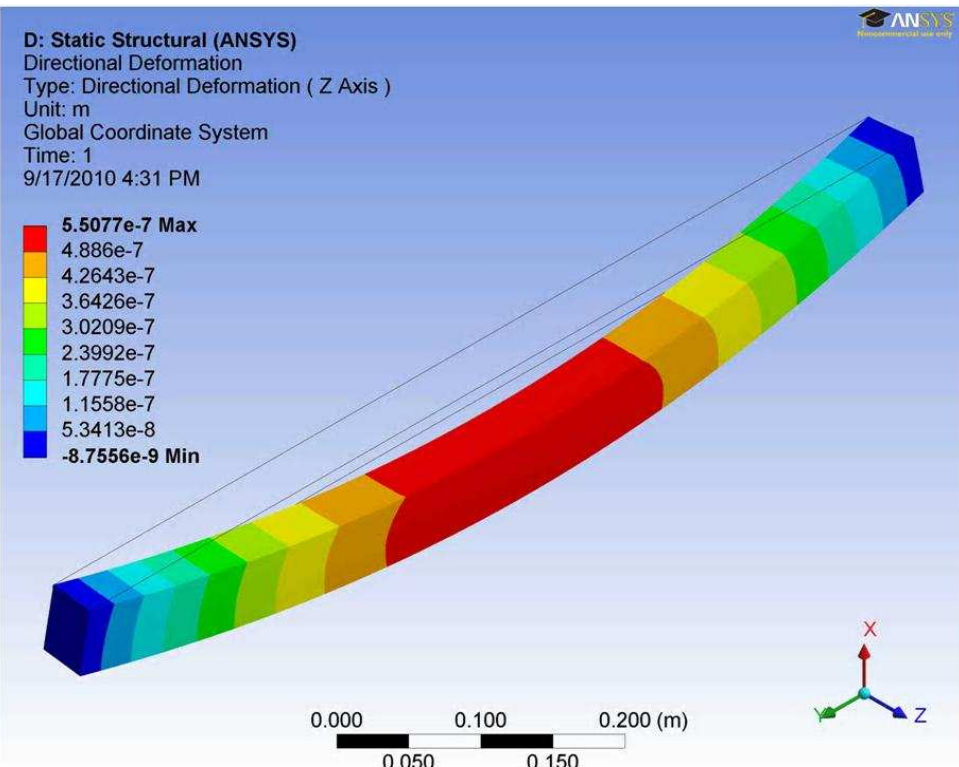
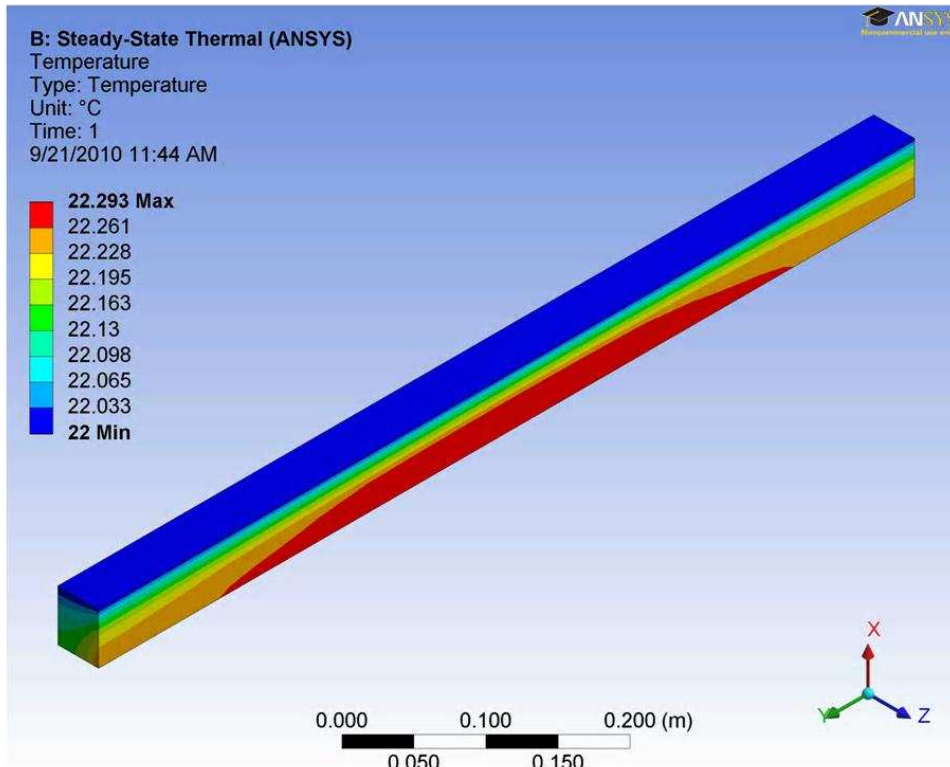


Single cooling surface

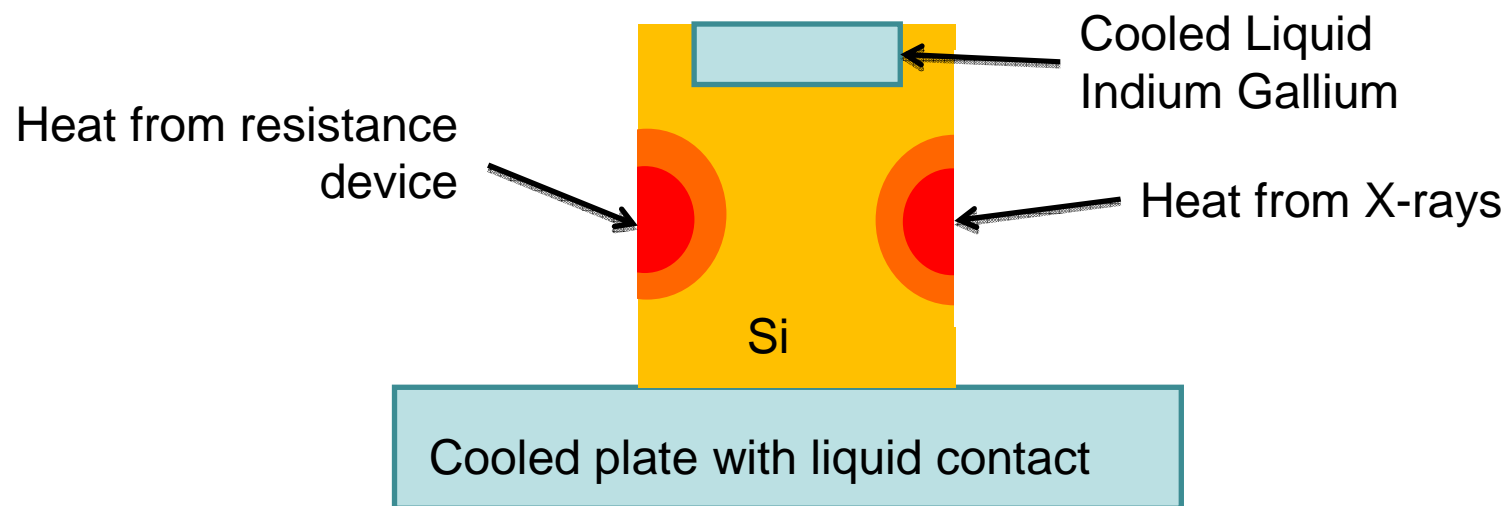


Michael Weinbaum

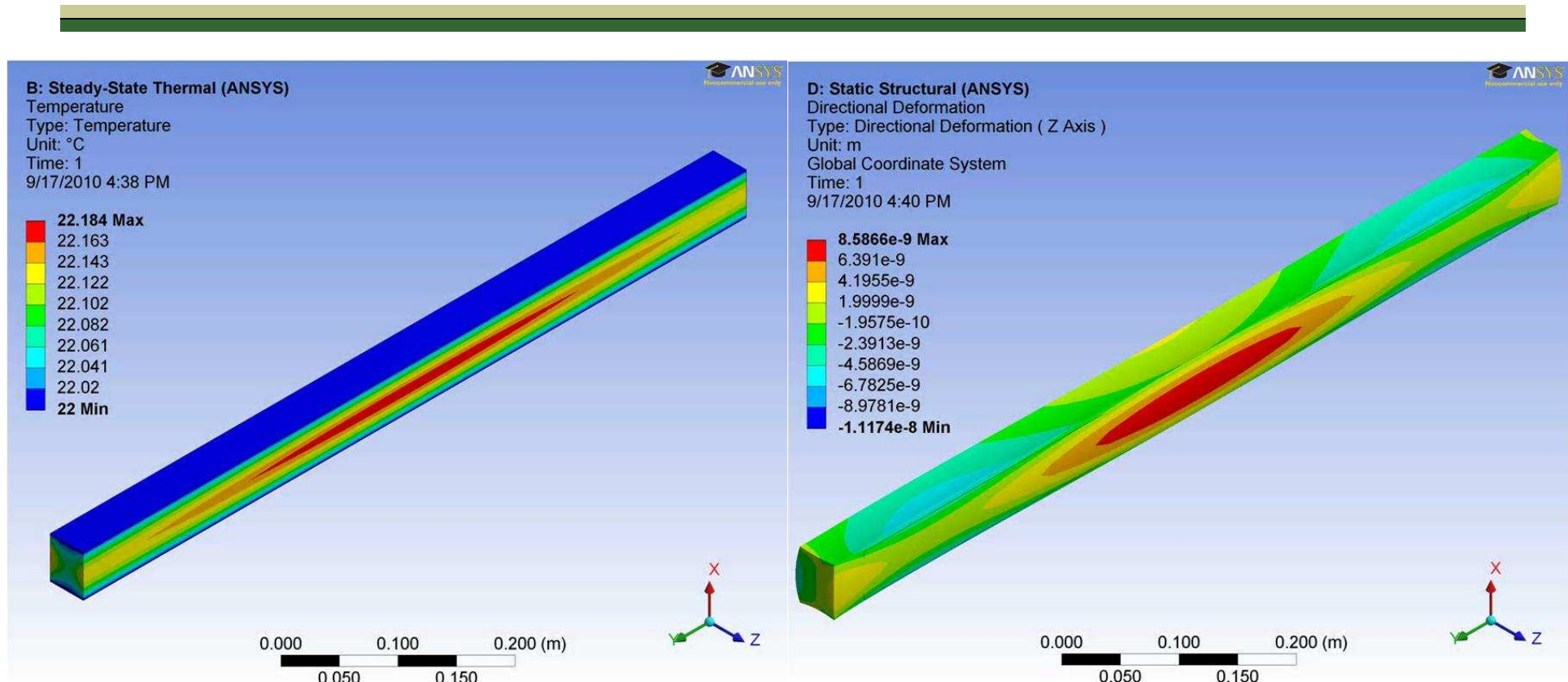
Single cooling surface only



Setup-backlight with two cooling surfaces

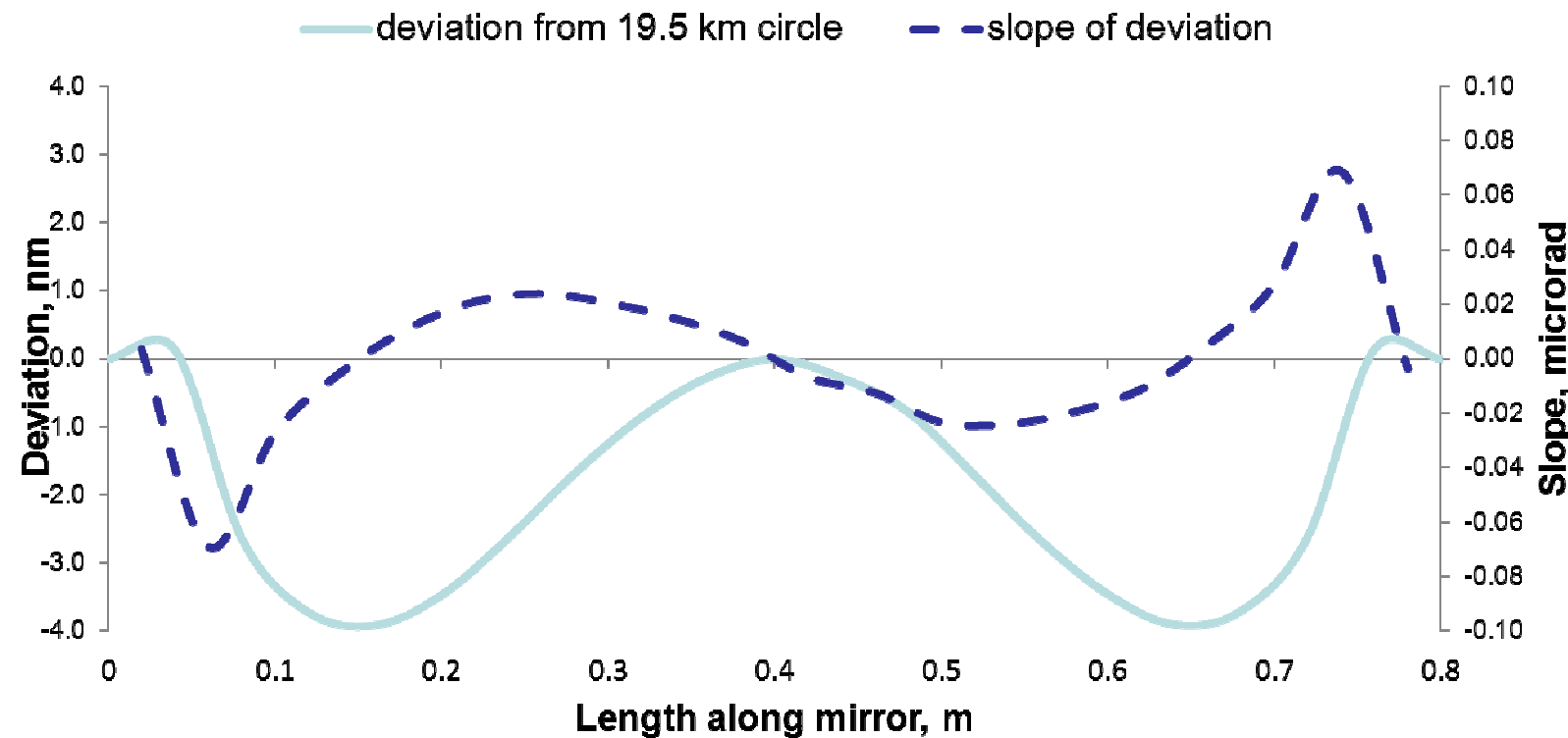


Results- backlighting with two cooling surfaces



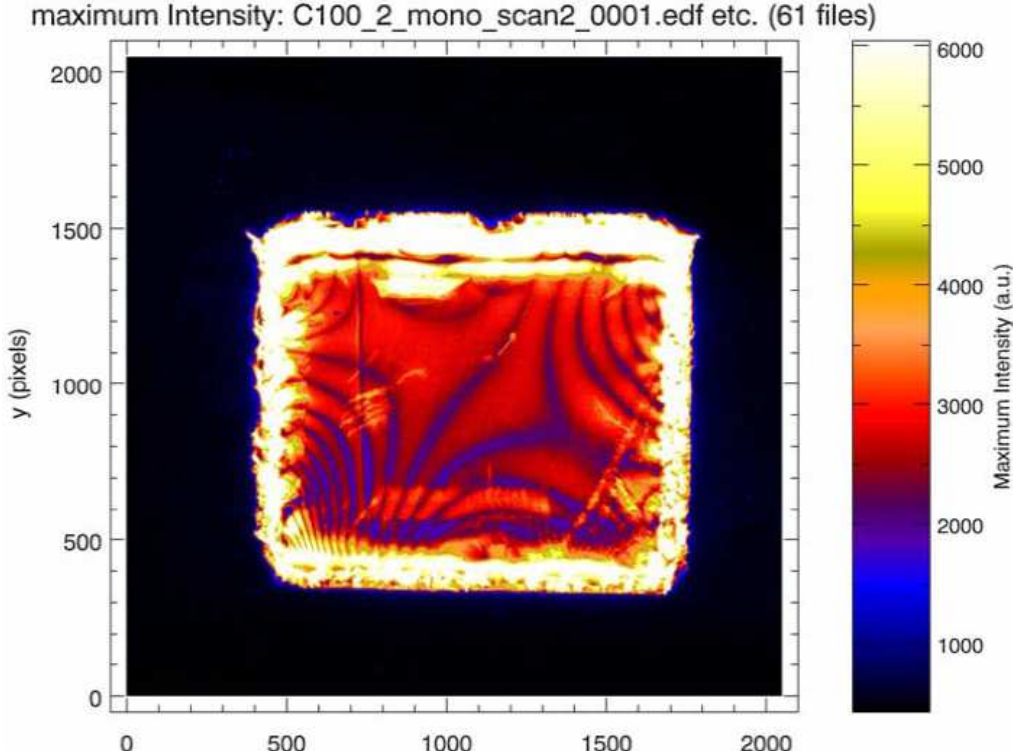
Order of magnitude lower distortion

Results – film and sym. cooling

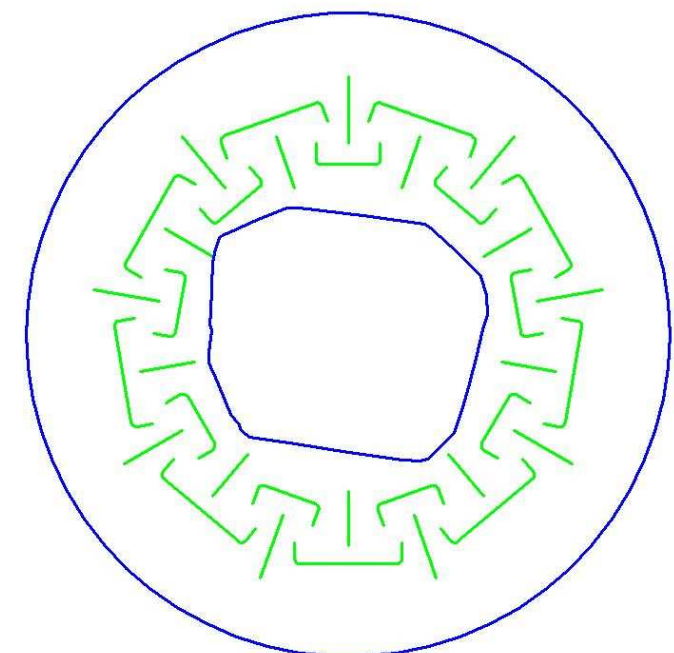


Simulation included 100 micron tungsten film with a 36K temperature change

Stress relief in diamond/CVD ring monochromator



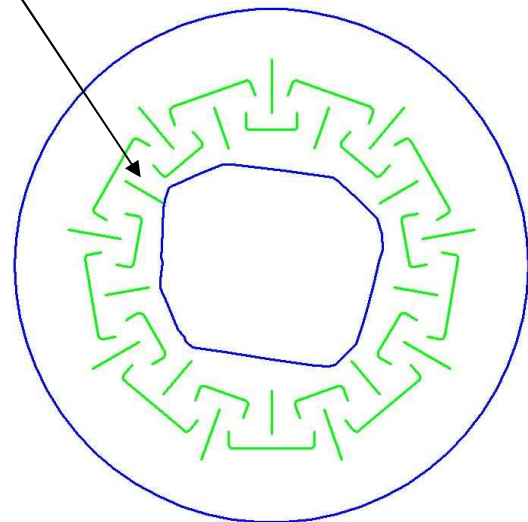
Growers proposed cuts



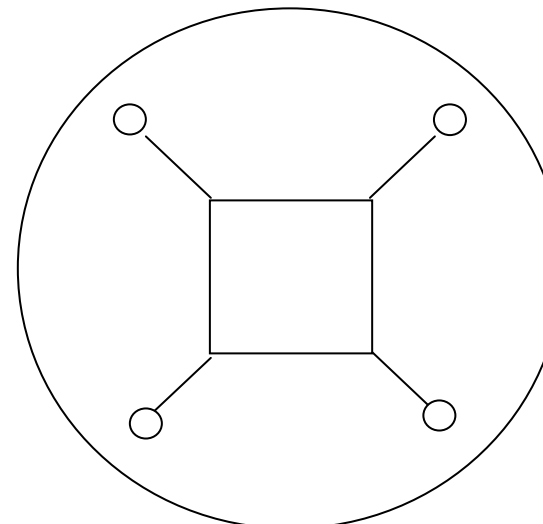
Liubov Samoylova, XFEL

Diamond Monochromator Stress Relief

Useful cut



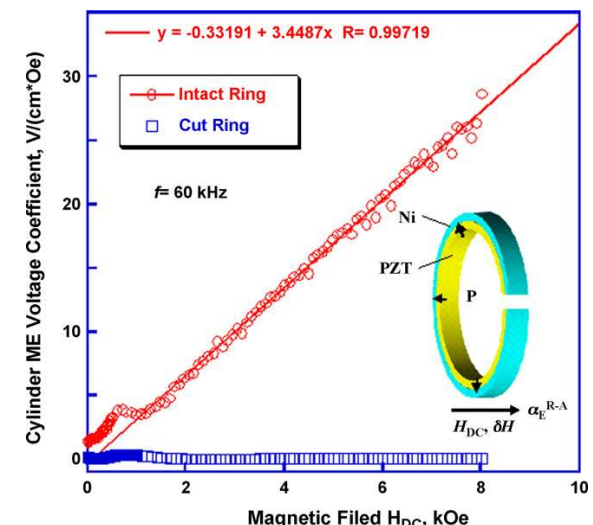
vs.



Fan Yang, XFEL

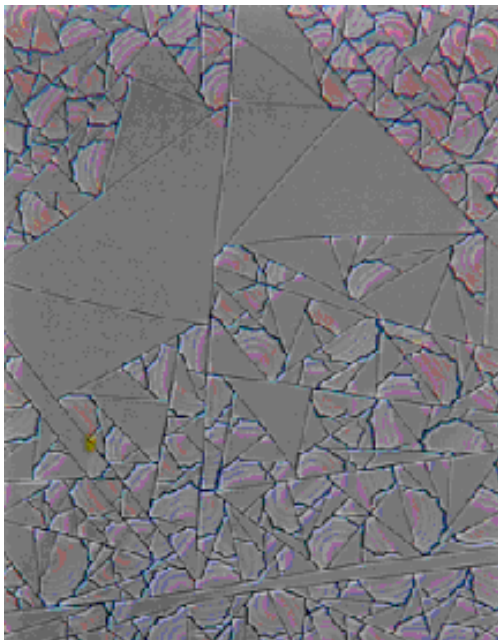
Hoop (circumferential) stress relief σ_θ for a cut ring

Geometry Effects on Magnetoelectric Performance of Layered Ni/PZT Composites,
D.A. Pan, J.J. Tian, S.G. Zhang, J.S. Sun, A.A. Volinsky, L.J. Qiao, Mater. Sci.
Eng. B, Vol. 163(2), pp. 114-119, 2009

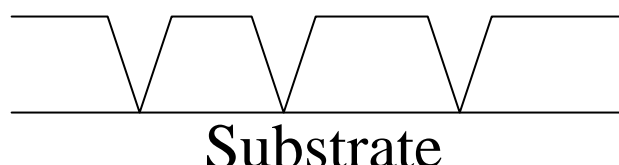


Stress Relief Through Fracture

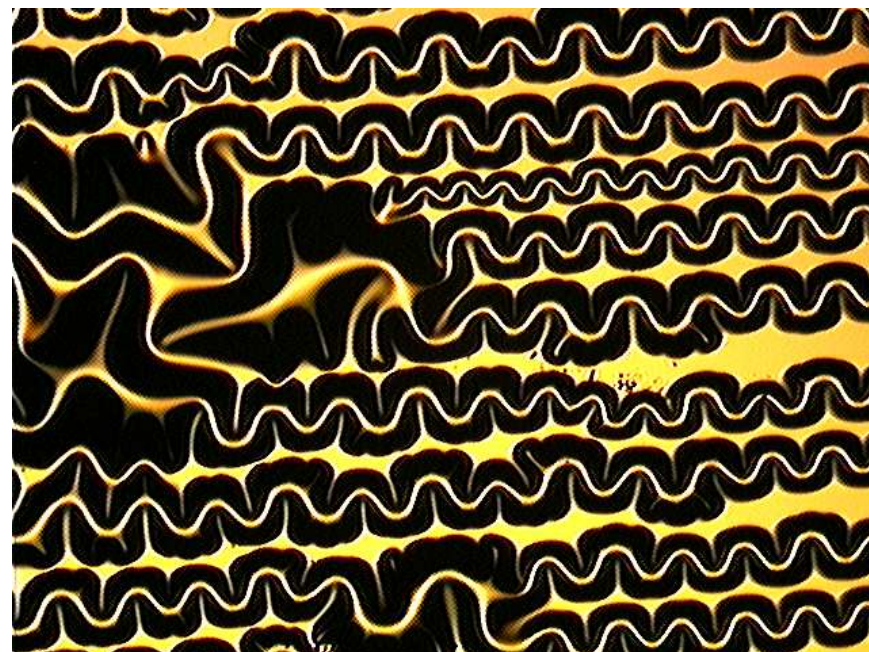
Low-K dielectric film
fracture in tension



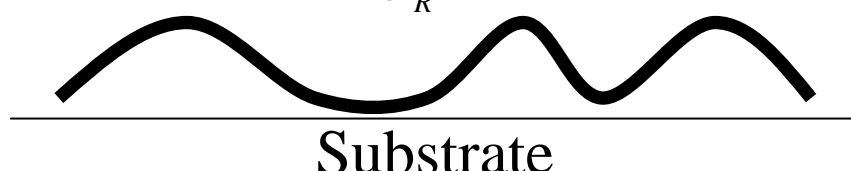
$$h_c = \frac{K^2}{Z\sigma_R^2}$$



TiW film phone cord delamination in
compression



$$h_c = \frac{GE}{Z\sigma_R^2}$$



Mechanics of Coating Fracture

The strain energy release rate of a stressed coating:
(i.e. amount of energy stored in a stressed coating per unit area, J/m², *stressed coating is comparable to a loaded spring*)

Coating will delaminate when the strain energy release rate equals the interfacial toughness, $\Gamma_i(\Psi)$, or its adhesion:

$$G = \Gamma_i(\Psi)$$

$$G = Z \frac{(1 - \nu_c^2) \sigma^2 t}{E_c}$$



The coating will crack when the strain energy release rate equals the coating toughness, $\Gamma_{coating}$:

$$G = \Gamma_{coating}$$

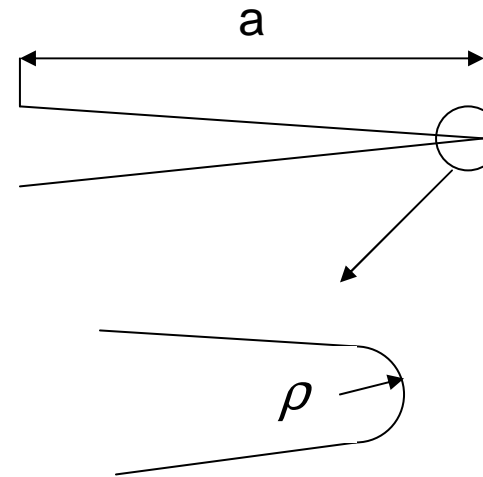


Stress Concentration

Stress at the crack tip is magnified by a factor:

$$\frac{\sigma_{crack\ tip}}{\sigma_{thermal}^{applied}} = C \sqrt{\frac{a}{\rho}}$$

Crack length Crack tip radius



For a 100 nm crack or defect with 1 nm tip radius, one would find a **10-fold increase** in the stress levels at the crack tip.

Thermal Stress Mechanics

Thermal stress in the coating: $\sigma_{thermal} = \frac{E_c}{1-\nu_c} (\alpha_c - \alpha_s) \cdot \Delta T$

$$G = Z \frac{(1+\nu_c) E_c (\alpha_c - \alpha_s)^2 \Delta T^2 t}{(1-\nu_c)}$$

Thermal expansion mismatch causes substantial substrate bending!

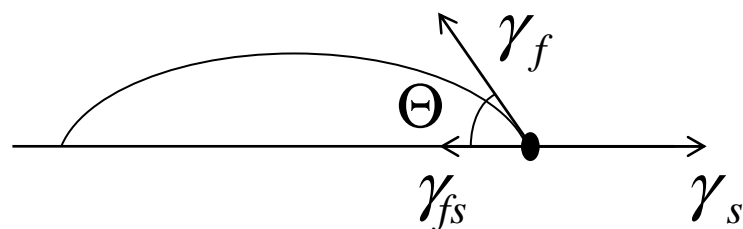


Work of Adhesion

Total irreversible energy per unit area of delamination extension required to separate the materials at the interface.

Thermodynamic work of adhesion

$$W_A = \gamma_f + \gamma_s - \gamma_{fs} = \gamma_f(1 + \cos\Theta)$$

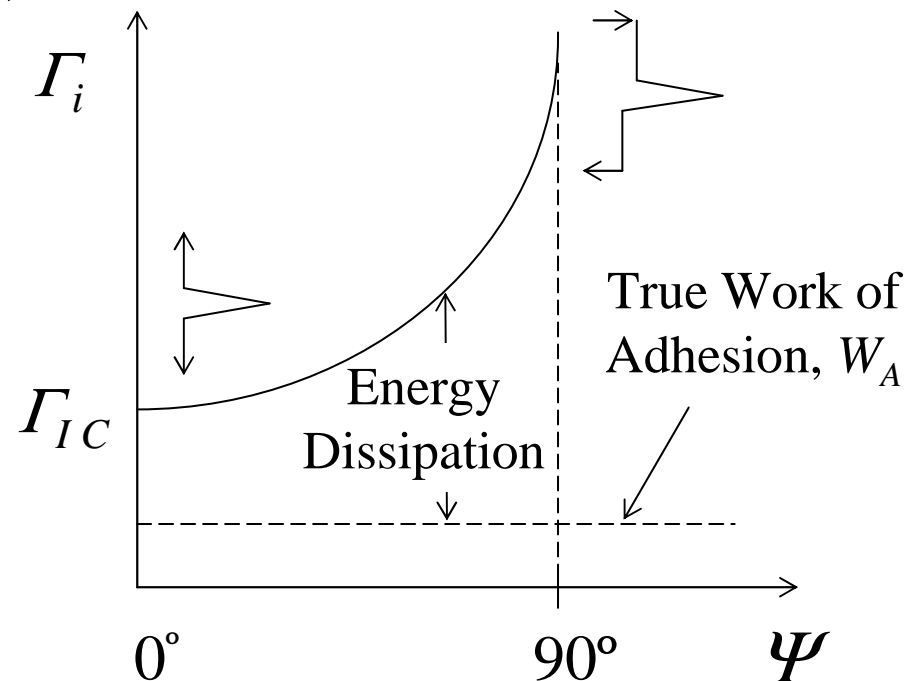


$$G = -\frac{dU_M}{dA} \quad G \geq \Gamma_i(\Psi)$$

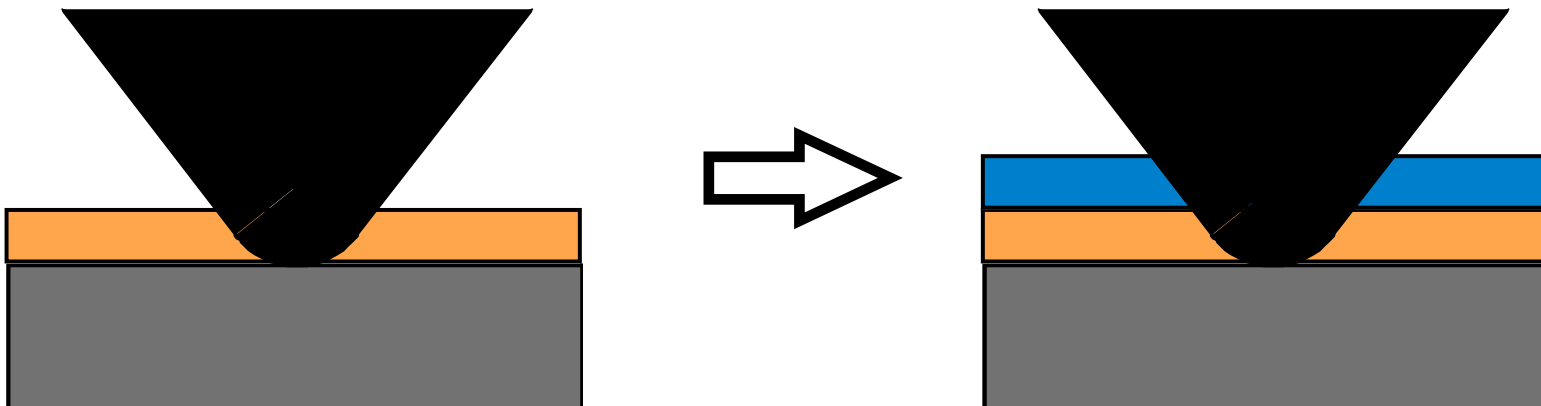
$$\Psi = \tan^{-1}(\tau/\sigma)$$

Practical work of adhesion

$$W_{A,P}(W_A) = W_A + U_f + U_s$$



Single Layer vs. Superlayer Indentation



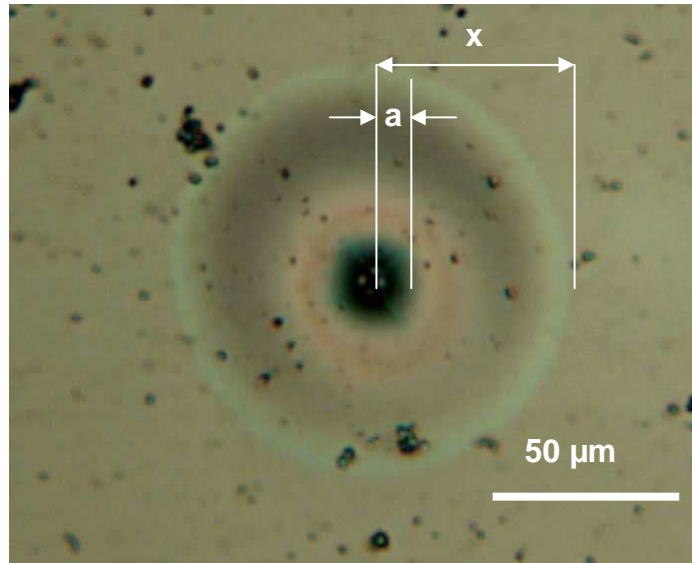
$$\frac{GE_f}{(1-\nu_f)} = \frac{1}{2} h \sigma_I^2 (1 + \nu_f) + (1 - \alpha)(h \sigma_R^2) - (1 - \alpha)h(\sigma_I - \sigma_B)^2$$

Nonbuckled: $\alpha = 1$, Buckled (single,double): $0 < \alpha < 1$

Biaxial Film Stress Relation: $\sigma = \epsilon E/(1-\nu)$

1. D.B. Marshall and A.G. Evans, Measurement of adherence of residually stressed thin films by indentation. I. Mechanics of interface delamination, *J. Appl. Phys.*, **56** (1984) p. 2632-2638.
2. J.W. Hutchinson and Z. Suo, Mixed mode cracking in layered materials, in *Advances in Applied Mechanics*, 1992, Academic Press, Inc.: New York, p. 63-169.
3. M.D. Kriese and W.W. Gerberich, Quantitative adhesion measures of multilayer films. *J. Mater. Res.* **14** (7), p. 3007, 1999

Experimental Measurements

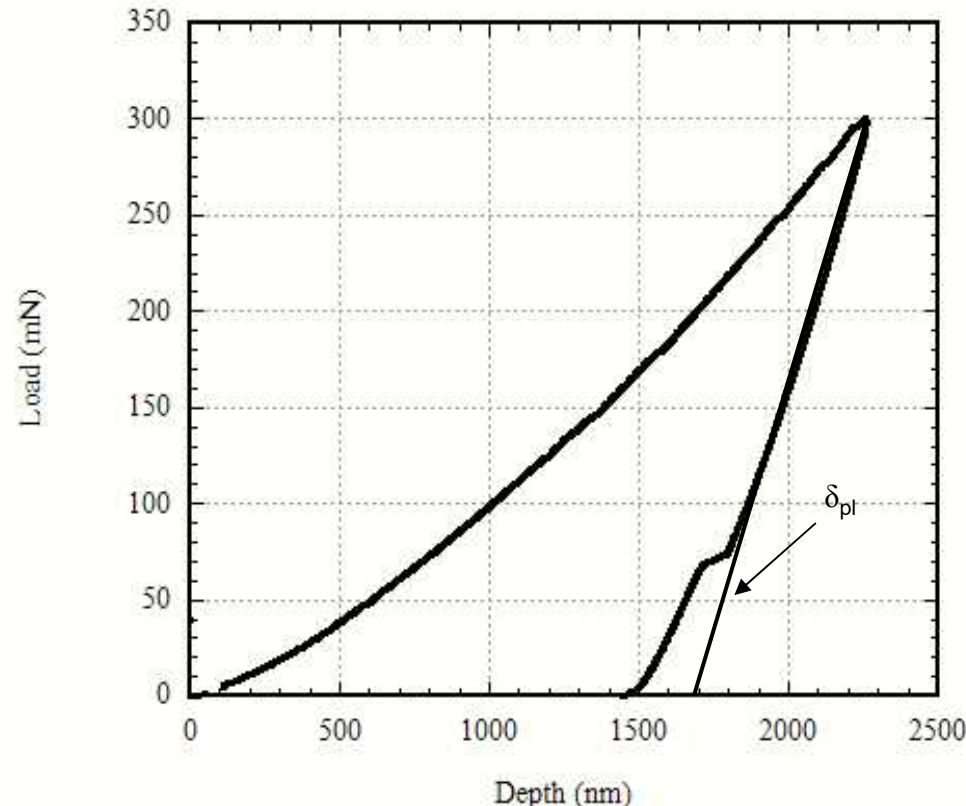


Optical Microscope used for
blister measurements

x = blister radius

a = contact radius of indenter tip

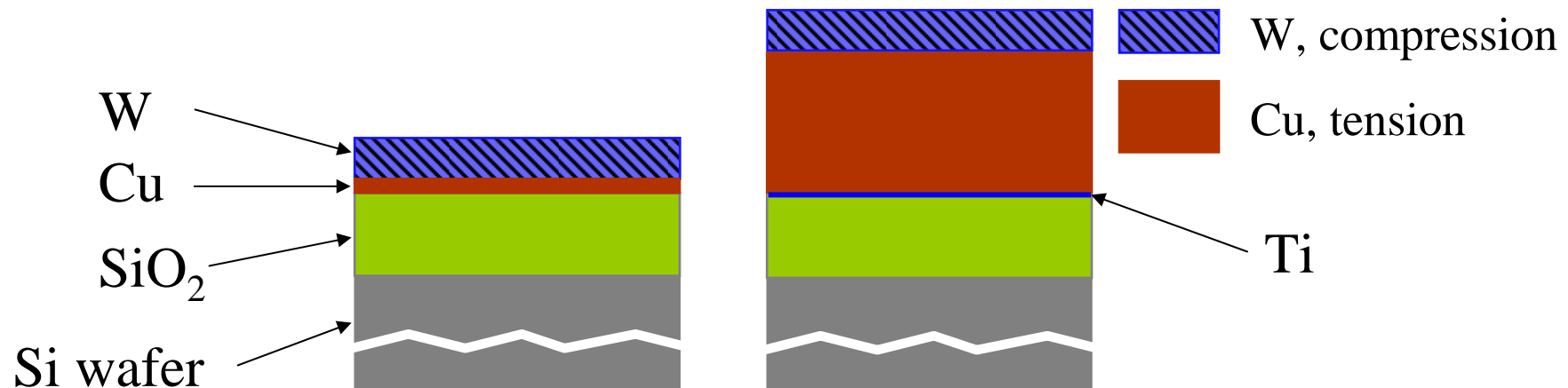
δ_{pl} = plastic indentation depth



Load-Displacement curve from the indenter

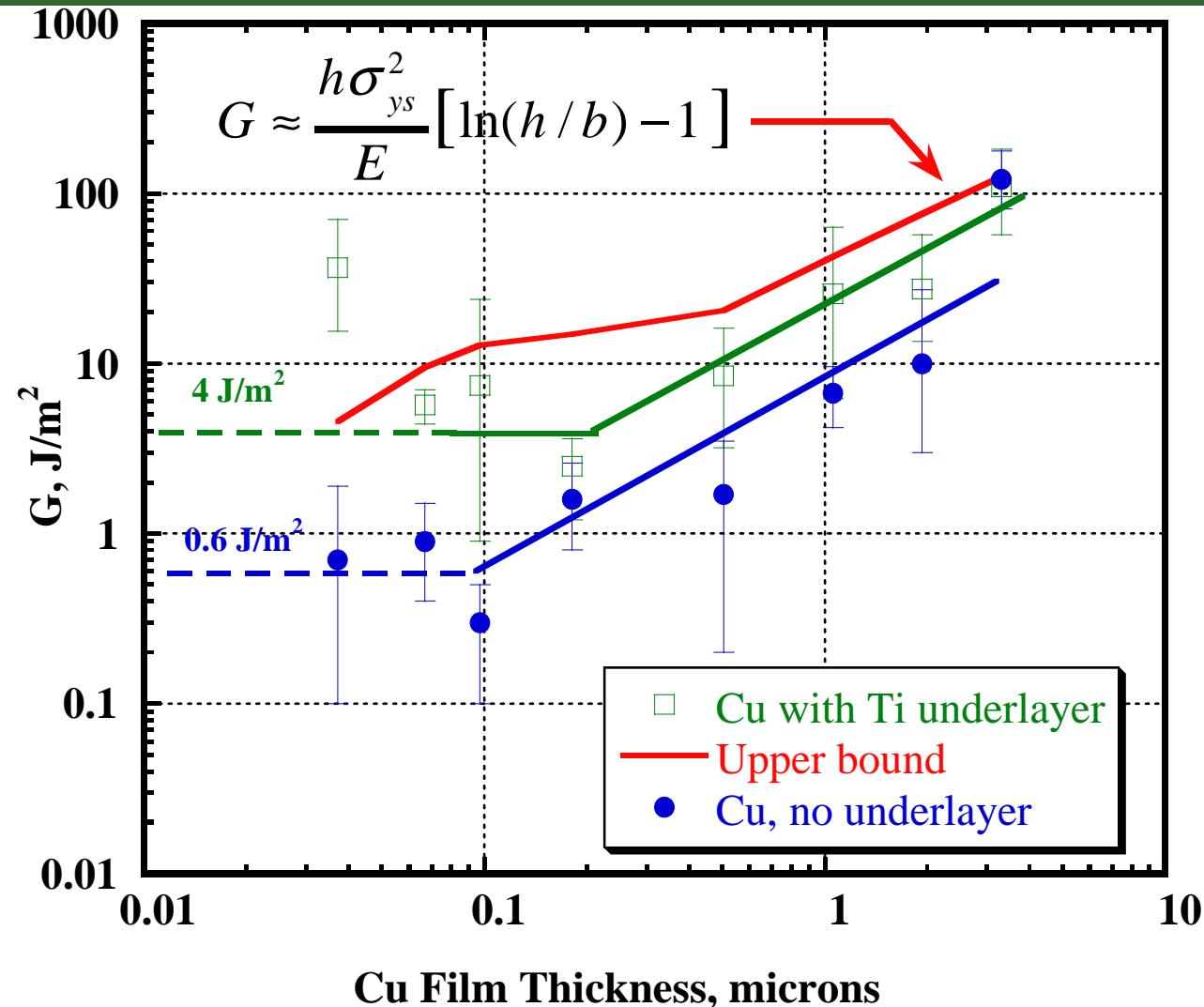
Cu-BASED THIN FILM SYSTEM

Films: 1 μm W overlayer on top of Cu films (40 nm to 3 μm)
with and without a 10 nm Ti underlayer



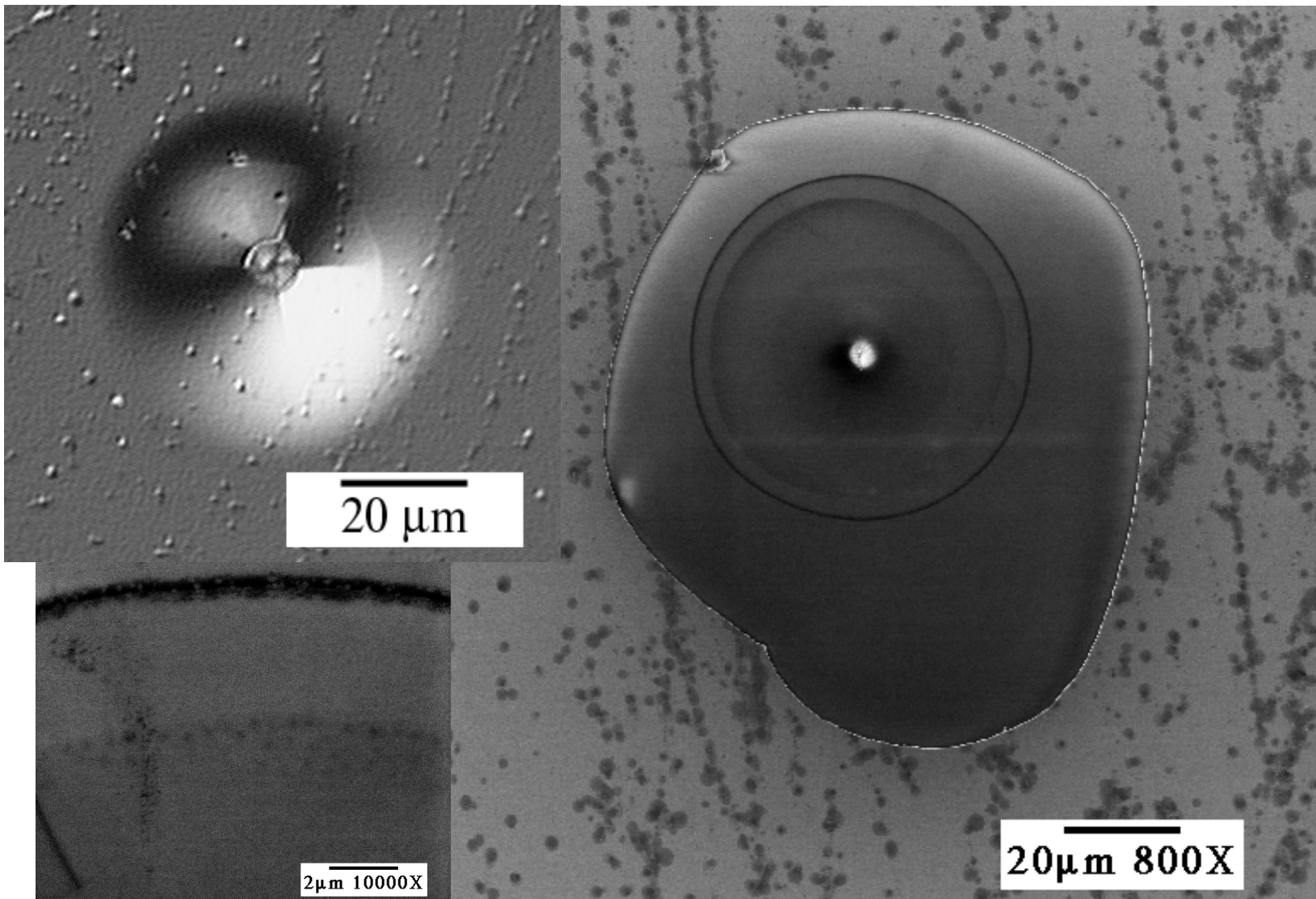
- **Substrates:** Si wafers $<100>$ w/ thermally grown 1.5 μm of SiO_2
- **Processing:** Cleanroom, sputtering in argon (1 μTorr pump down), no etching.

Cu Film Adhesion

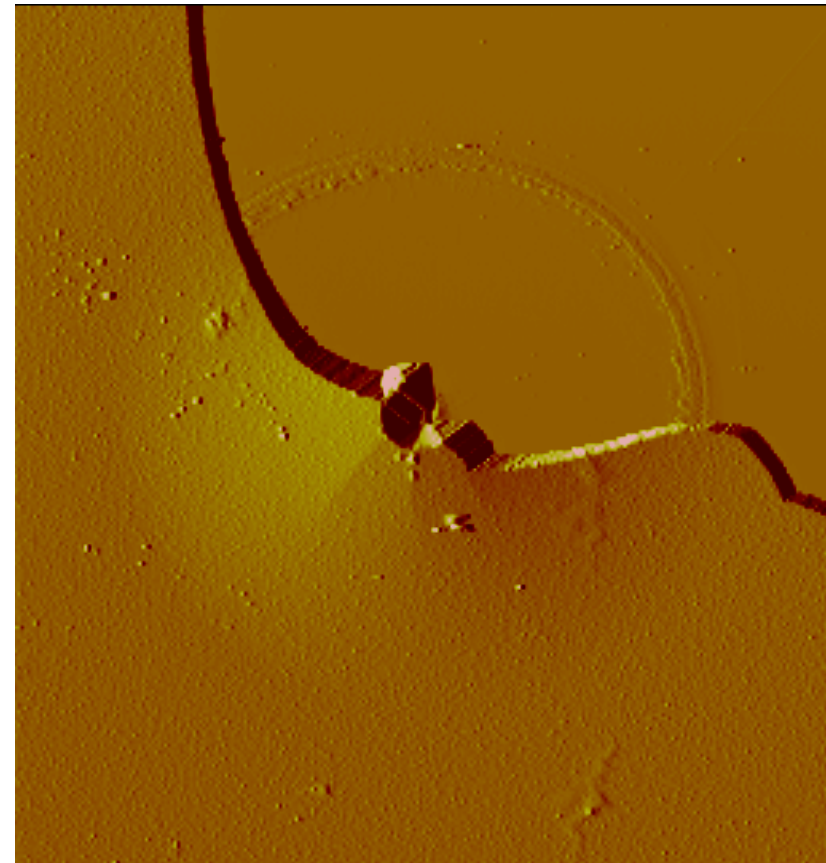
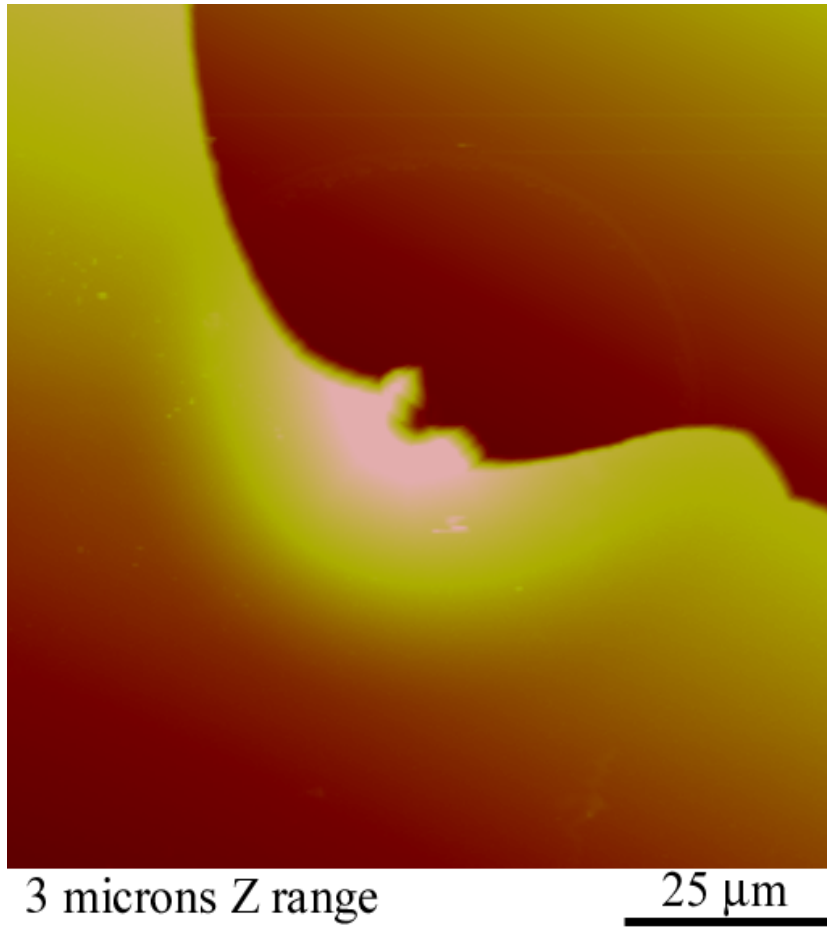


A.A. Volinsky, N.R. Moody, W.W. Gerberich, Acta Mater. Vol. 50/3, pp. 441-466, 2002

FIDUCIAL MARK. SEM

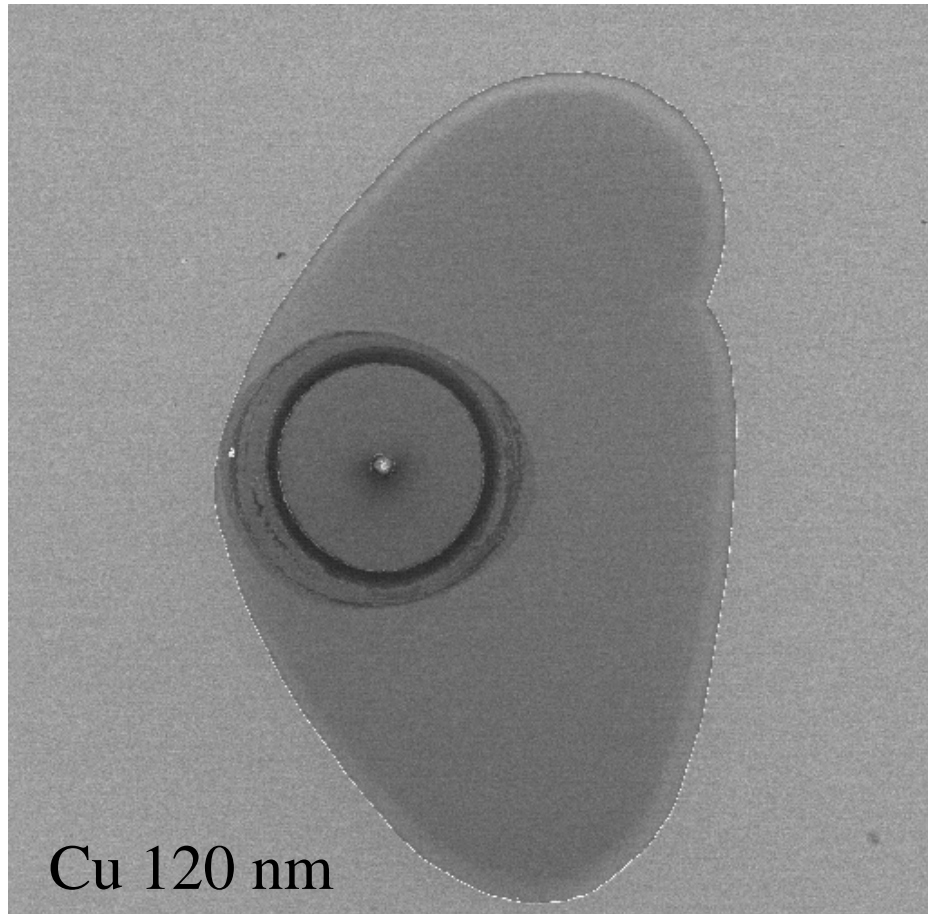


PARTIAL BLISTER REMOVAL



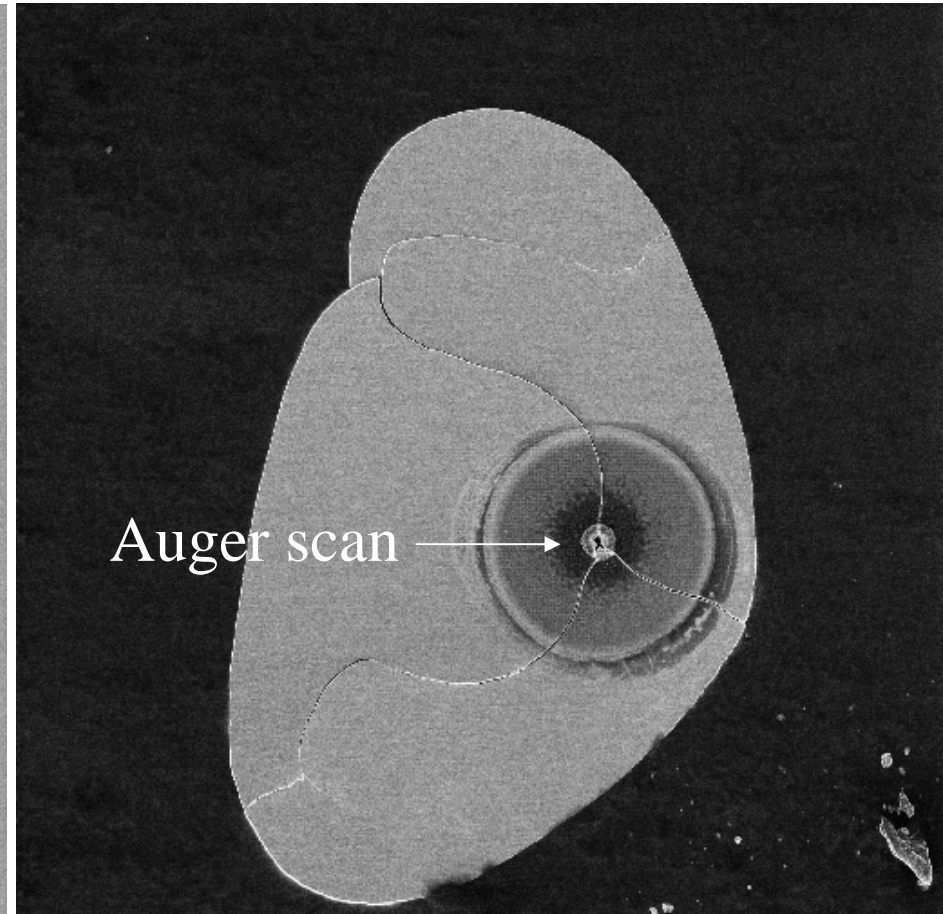
FIDUCIAL MARKS - SEM

Substrate (SiO_2) side



Cu 120 nm

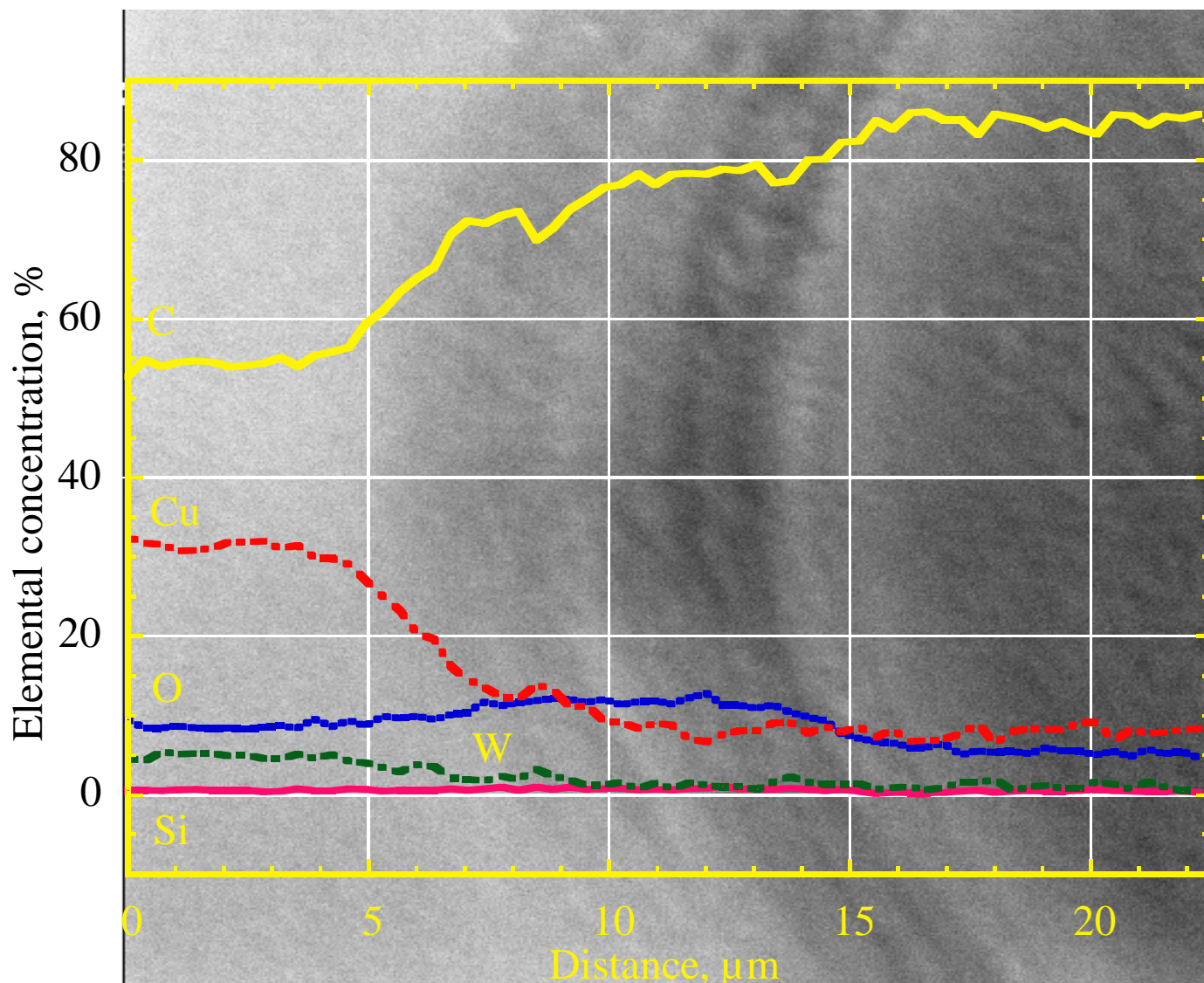
Sticky tape (Cu) side



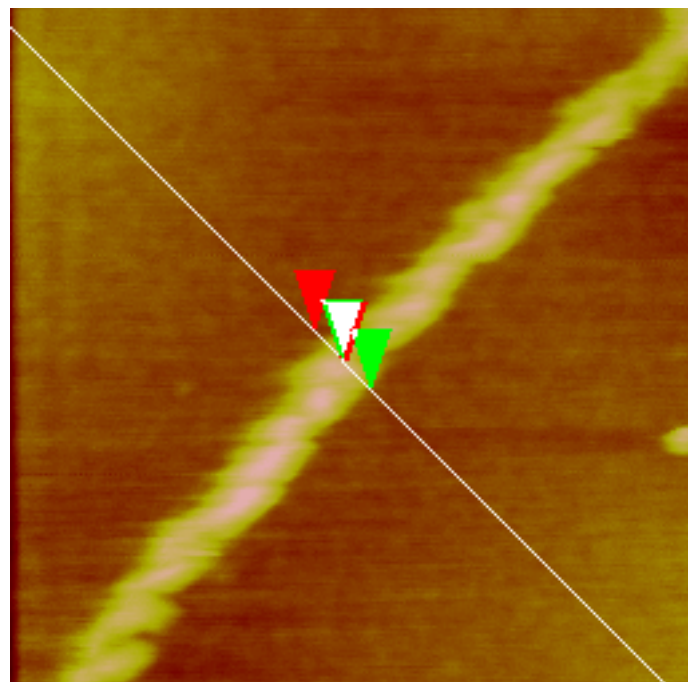
Alex A. Volinsky

www.eng.usf.edu/~volinsky

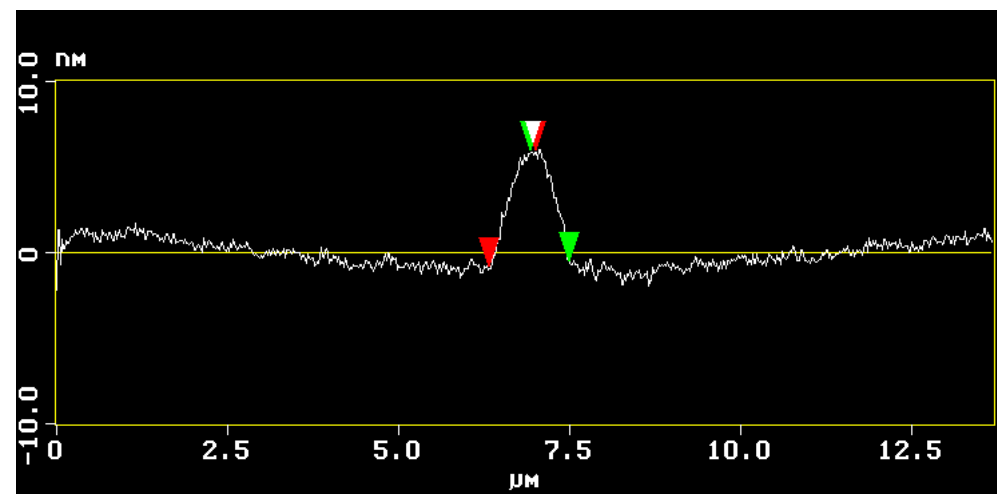
AES SCAN



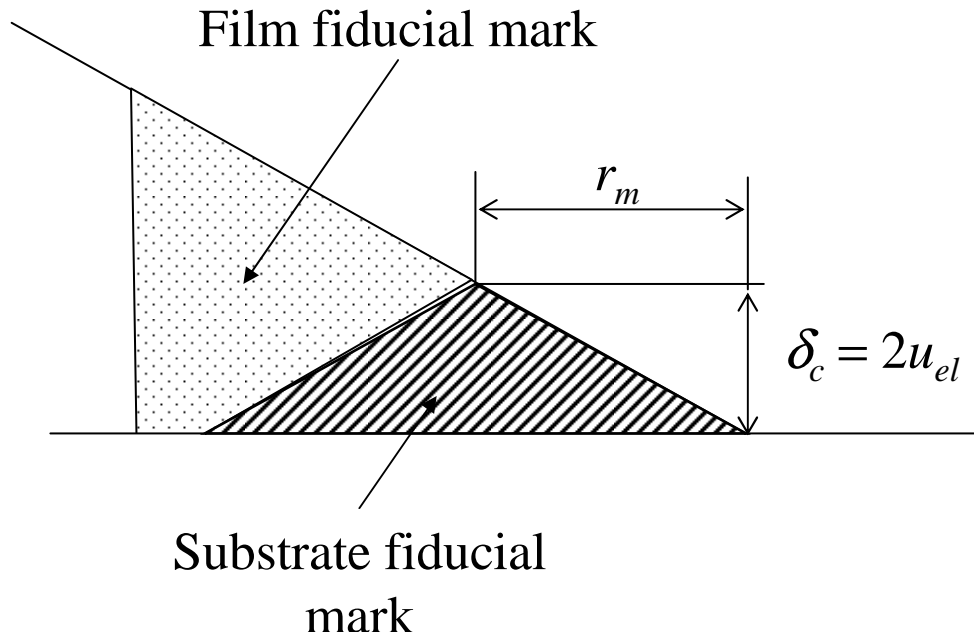
AFM MARK MEASUREMENTS



Surface distance	683.74 nm
Horiz distance(L)	683.59 nm
Vert distance	6.808 nm
Angle	0.571 deg
Surface distance	566.54 nm
Horiz distance	566.41 nm
Vert distance	6.473 nm
Angle	0.655 deg



LINEAR ELASTIC CRACK TIP ANALYSIS



$$u_{el}(r) = \frac{K}{E} \sqrt{\frac{8r}{\pi}}$$

Lawn B., (1993) "Fracture of Brittle Solids", Cambridge University Press, Cambridge

$$K_I = \delta_c E \sqrt{\frac{\pi}{32 r_m}}$$

$$K_I = 0.3 \text{ MPa}\cdot\text{m}^{1/2}$$

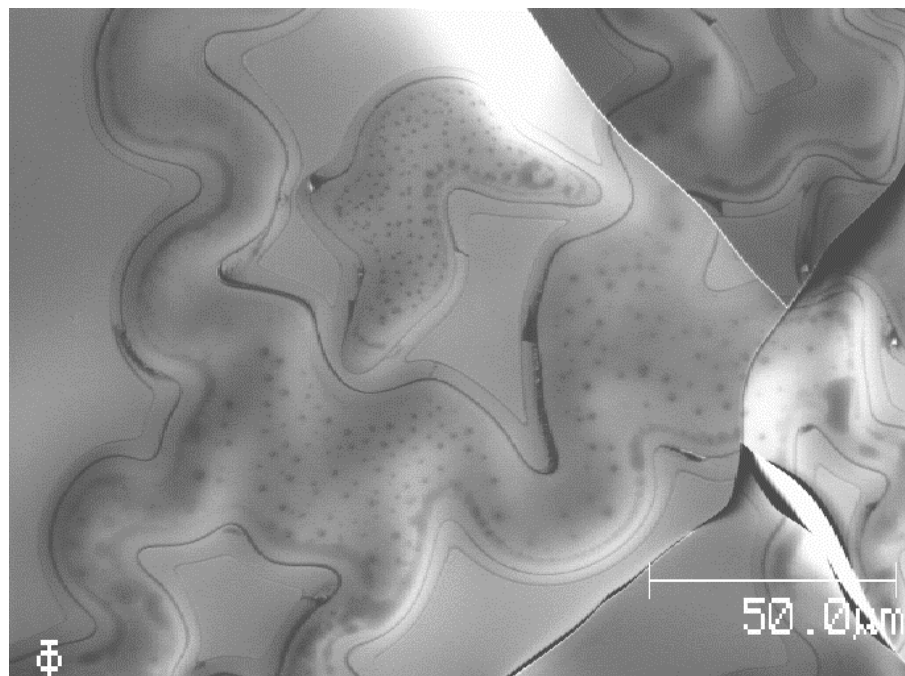
$$K_I = (G E)^{1/2}$$

$$G \approx 0.9 \text{ J/m}^2 \Rightarrow K_I = 0.33 \text{ MPa}\cdot\text{m}^{1/2}$$

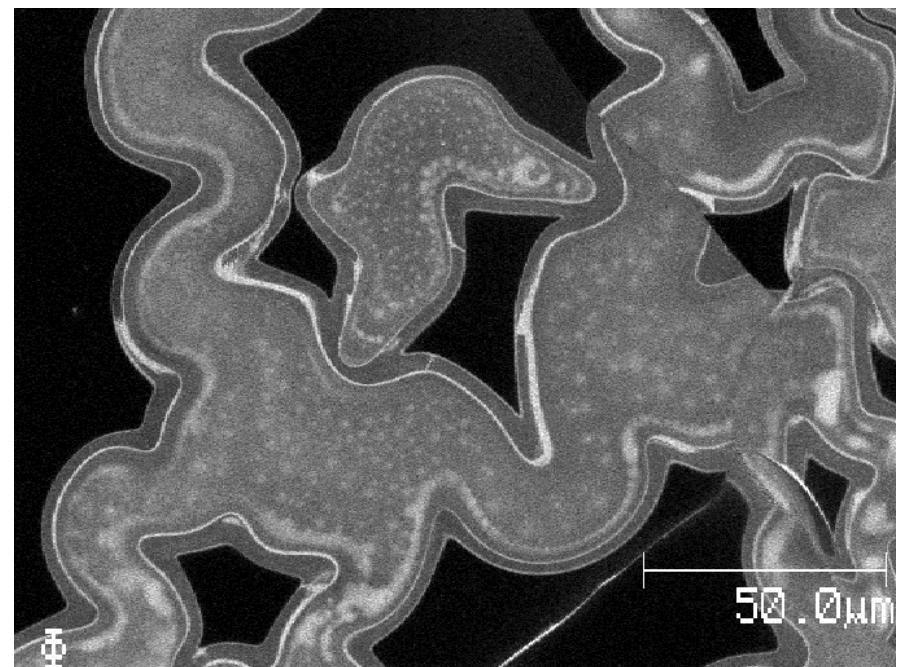
A.A. Volinsky, M.L. Kottke, N.R. Moody, W.W. Gerberich, Engineering Fracture Mechanics 69, pp. 1511-1515, 2002

Auger. Phone Cord Fiducial Marks

SEM



Carbon Map



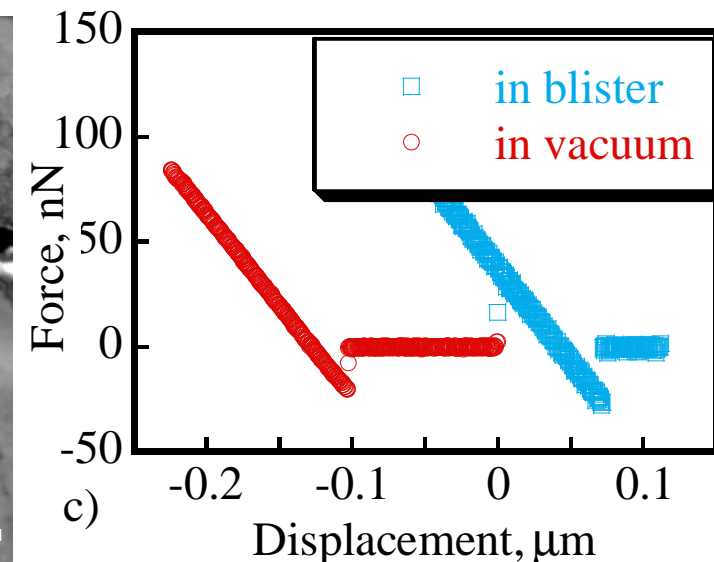
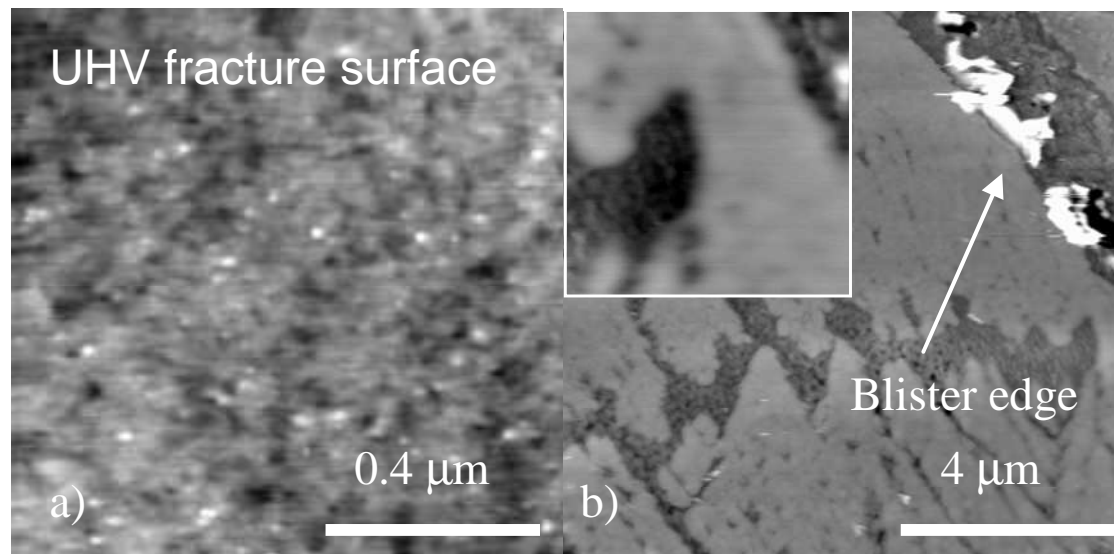
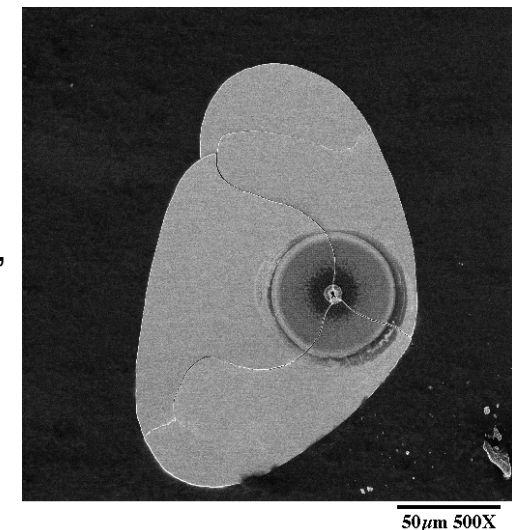
Mike Kottke

Crack Tip Surface Energy

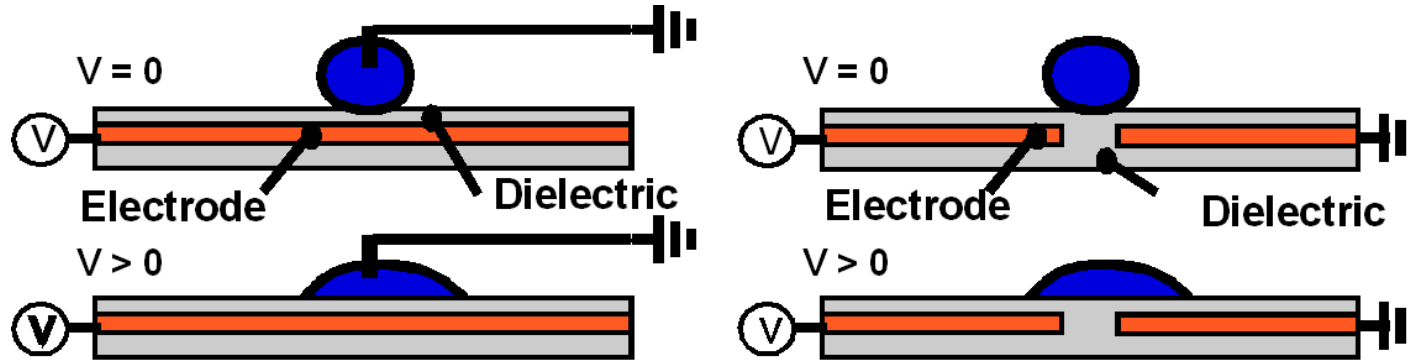
Conventional methods of surface energy measurement (contact angle technique) only work in air. While film is delaminating, its surface energy is reduced.

Fiducial Mark and Nanocrack Zone Formation During Thin Film Delamination,
A.A. Volinsky, N.R. Moody, M.L. Kottke, W.W. Gerberich, Philosophical Magazine A, Vol. 82, 2002

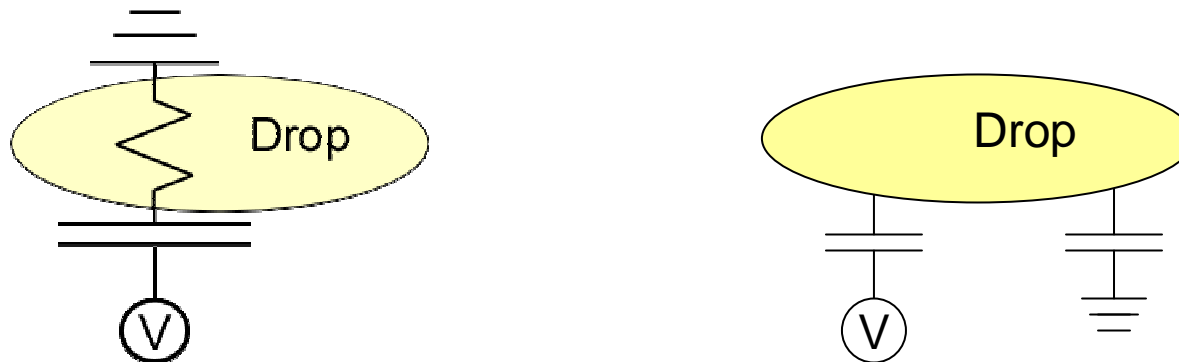
UHV-AFM (Prof. Szymonski's group). Create fracture surface in UHV, then use AFM tip pull-off data to calculate surface energy.



Electrowetting



Equivalent Electrical Circuit



Drops can be moved by varying electrical field around the drop

Electrowetting Measurement

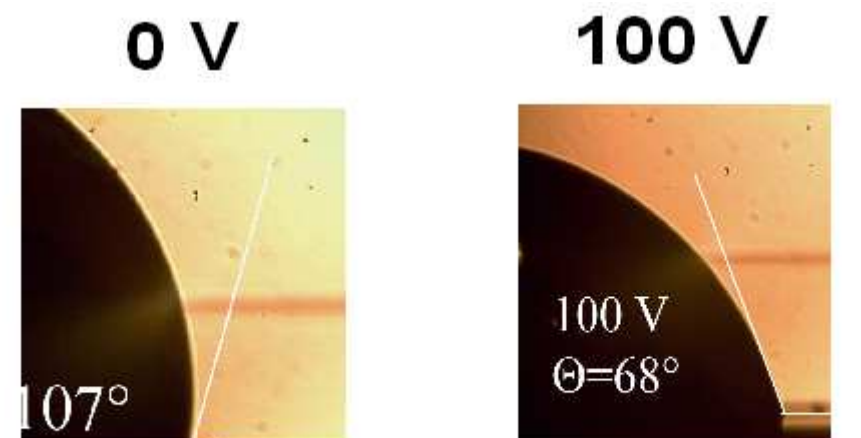
Electrowetting is typically characterized by the wetting angle

Fitted to Young-Lippman equation assuming parallel plate capacitor

Forces are estimated by modeling surface equilibrium

For many applications electrowetting force is of great interest:

Digital microfluidics, Adaptive cooling, focusing optics, flexible electronics, etc.

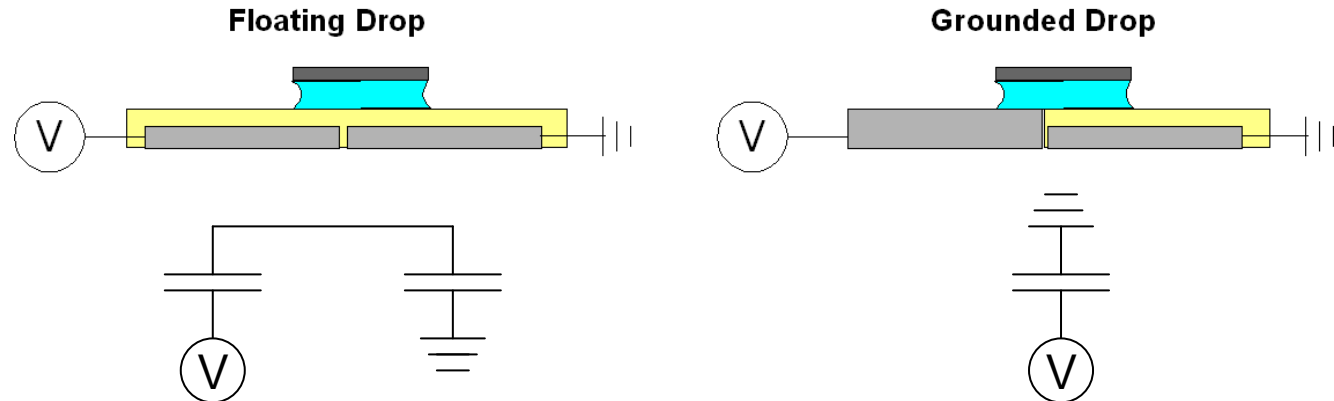


$\theta = 107 \text{ deg}$

$\theta = 68 \text{ deg}$

$$\cos \theta_1 = \cos \theta_o + \frac{\epsilon_o \epsilon_r V^2}{2 \gamma_{lv} \delta}$$

Electrowetting Configurations



Force-Position
(Lumped Parameter
Model)

$$E = \frac{V_{tot}^2 \epsilon_0 \epsilon_R}{8\delta} (s^2 - 4x^2)$$

$$F_x = \frac{dE}{dx} = -\frac{\epsilon_0 \epsilon_R}{\delta} V_{tot}^2 x$$

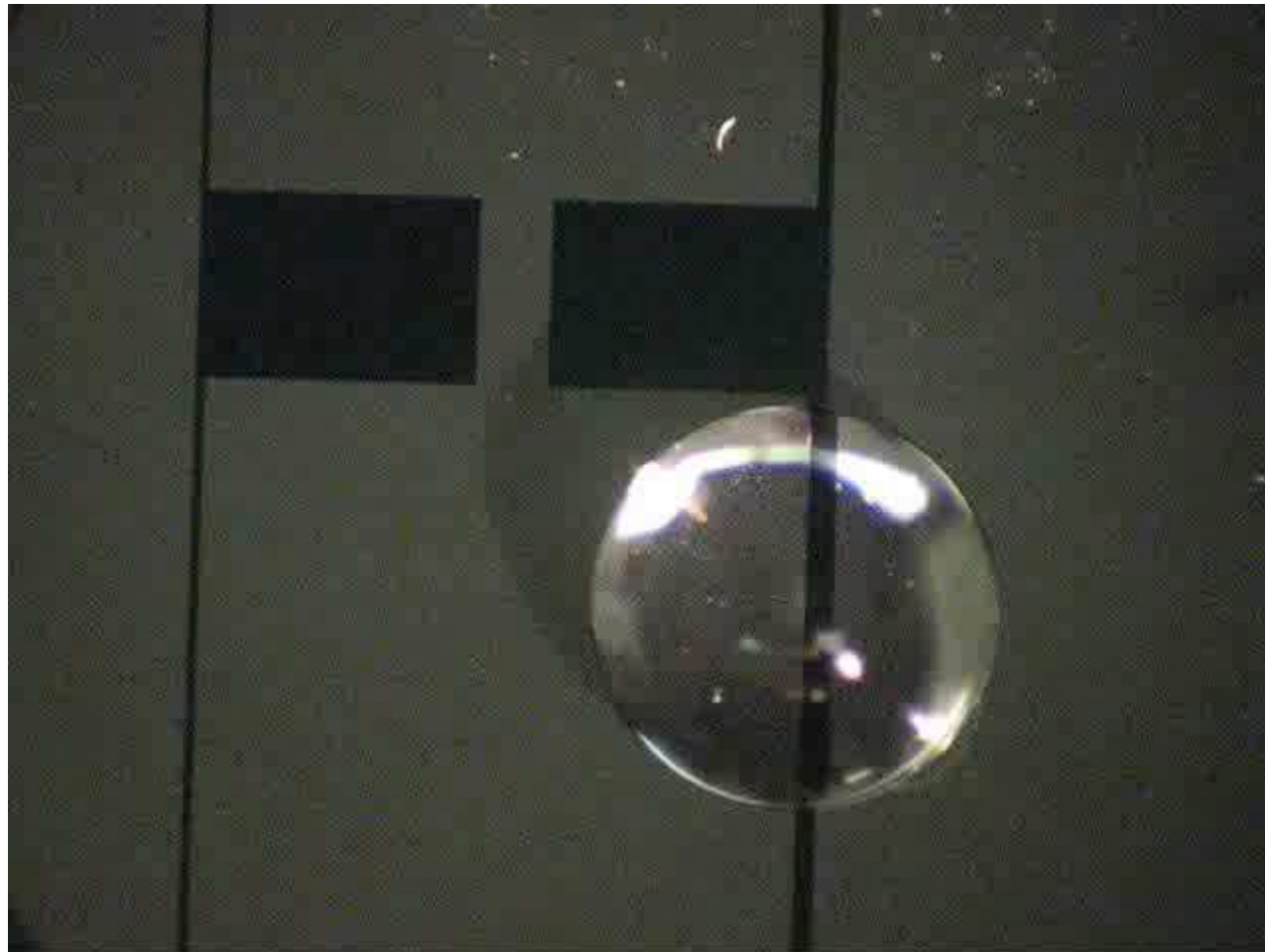
$$F_x = \frac{dE}{dx} = -\frac{\epsilon_0 \epsilon_R}{2\delta} s V_{tot}^2$$

s - edge length

x – plate displacement

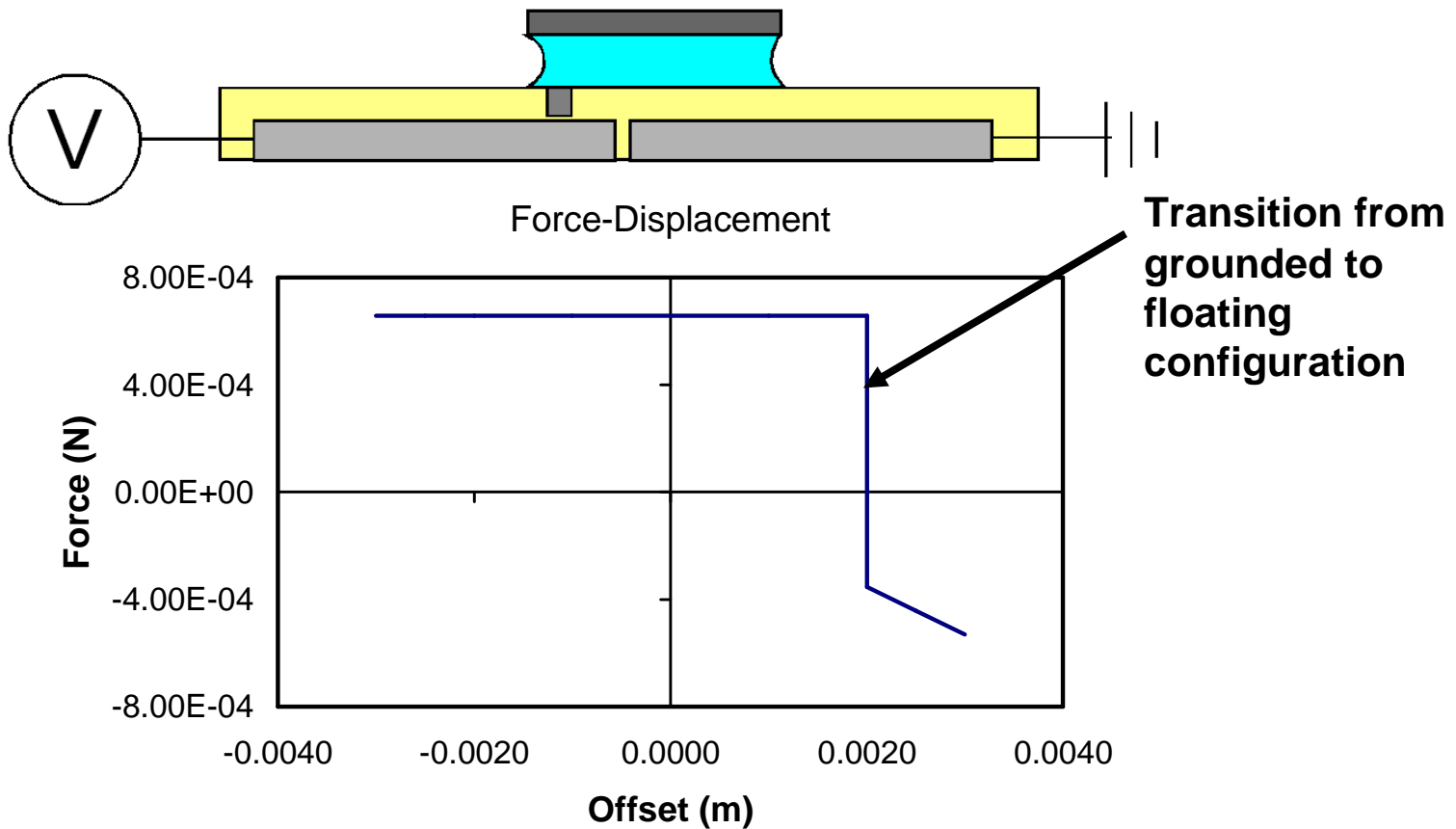
Forces are found by differentiating the system energy with respect to the appropriate displacement variable.

Electrowetting Oscillation. DC Voltage

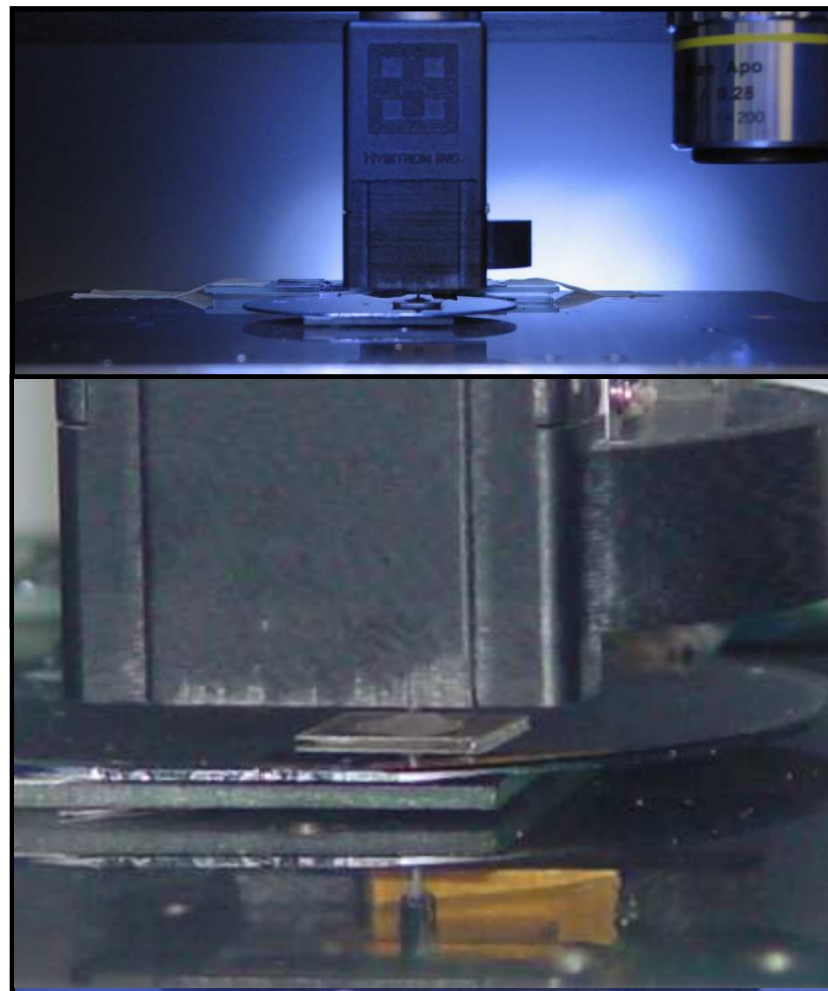
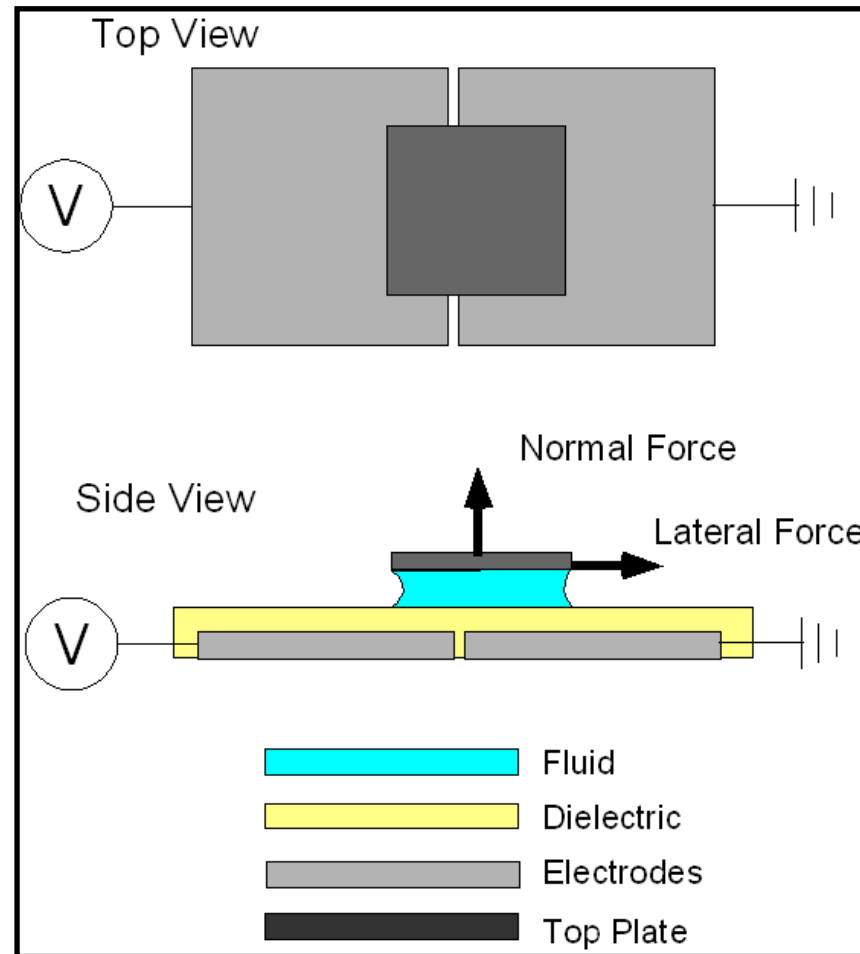


Oscillation Explanation: Local Dielectric Defect

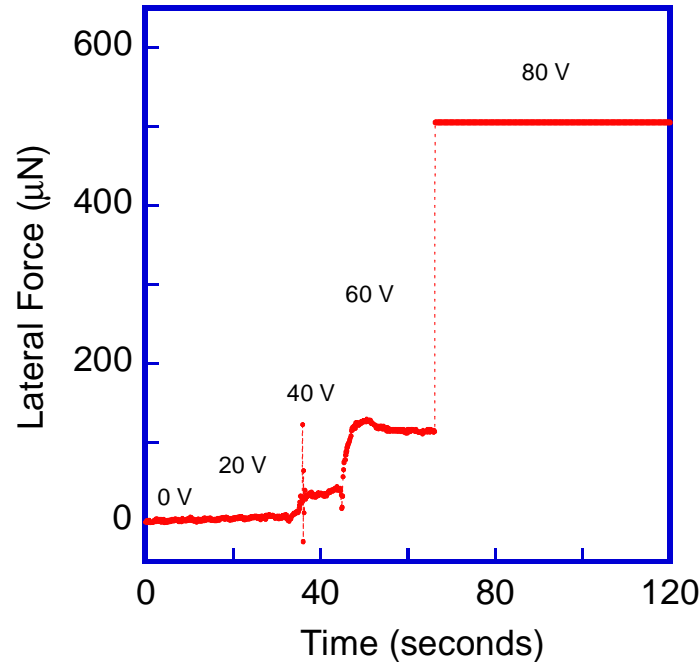
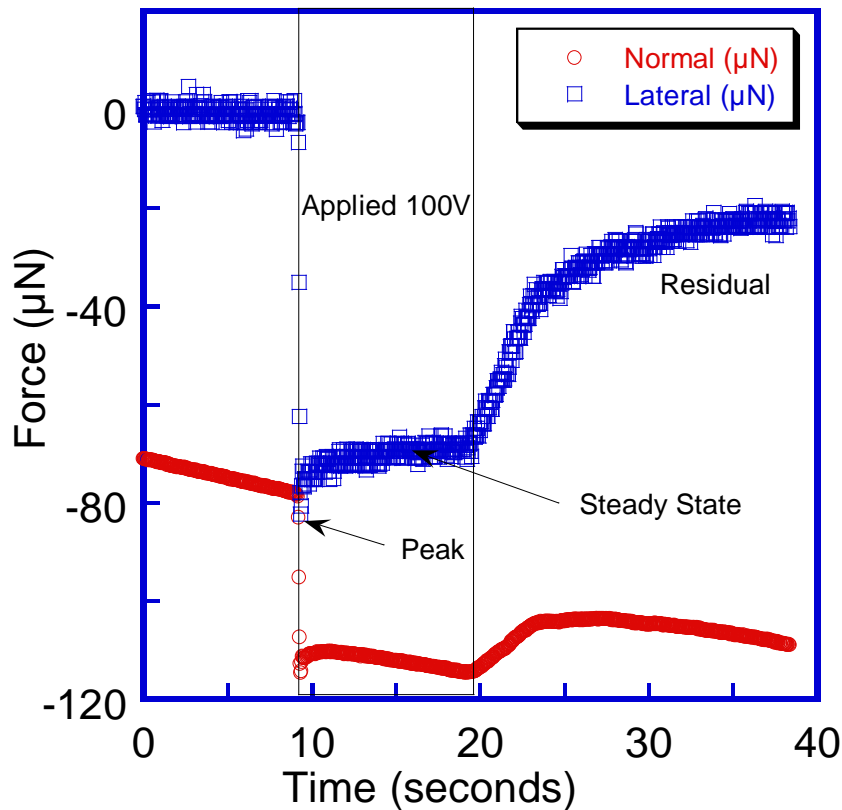
Dielectric Defect Results in Mixed-Mode Behavior



Force Measurement Configuration

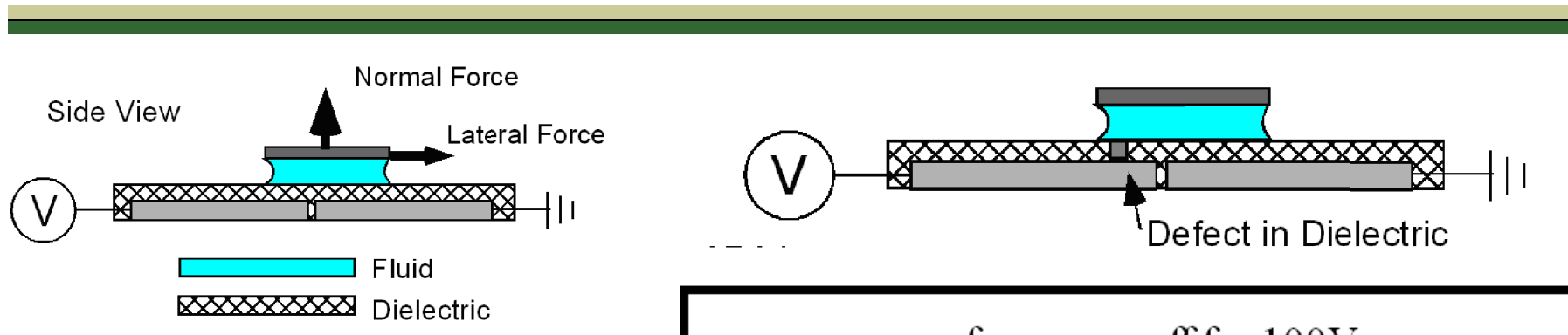


Typical Results



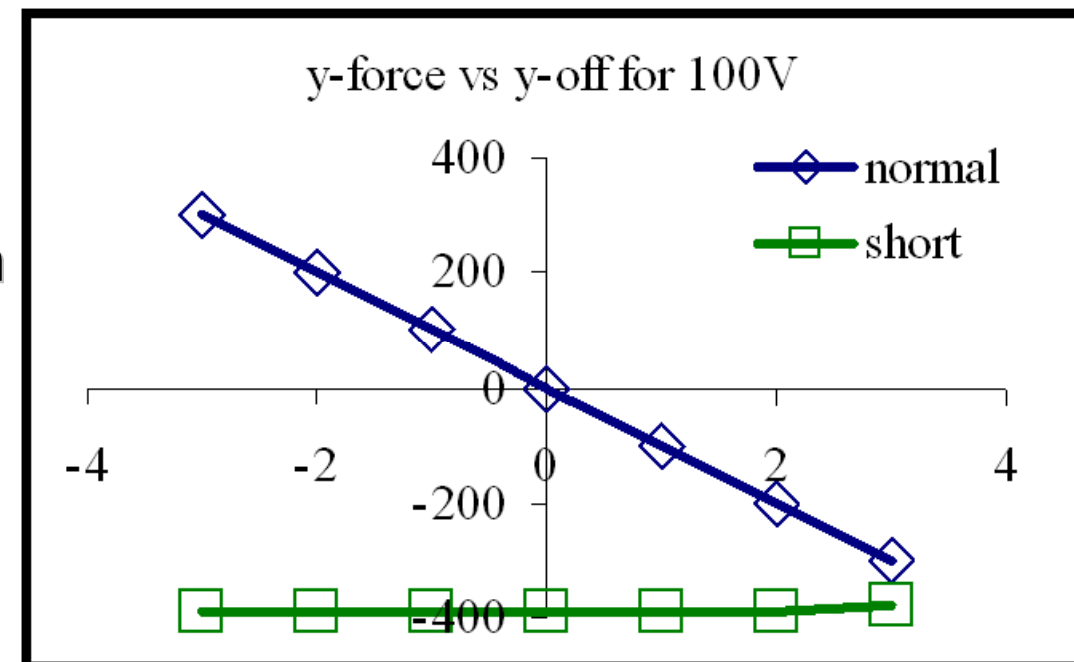
Applied Voltage (V)	Measured Force (μN)	Predicted Force (μN)	Prediction Method
20	6	11	Floating Drop
40	41	44	Floating Drop
60	113	98	Floating Drop
80	505	535	Grounded Drop

Y-force in a normal and defective dielectric layer

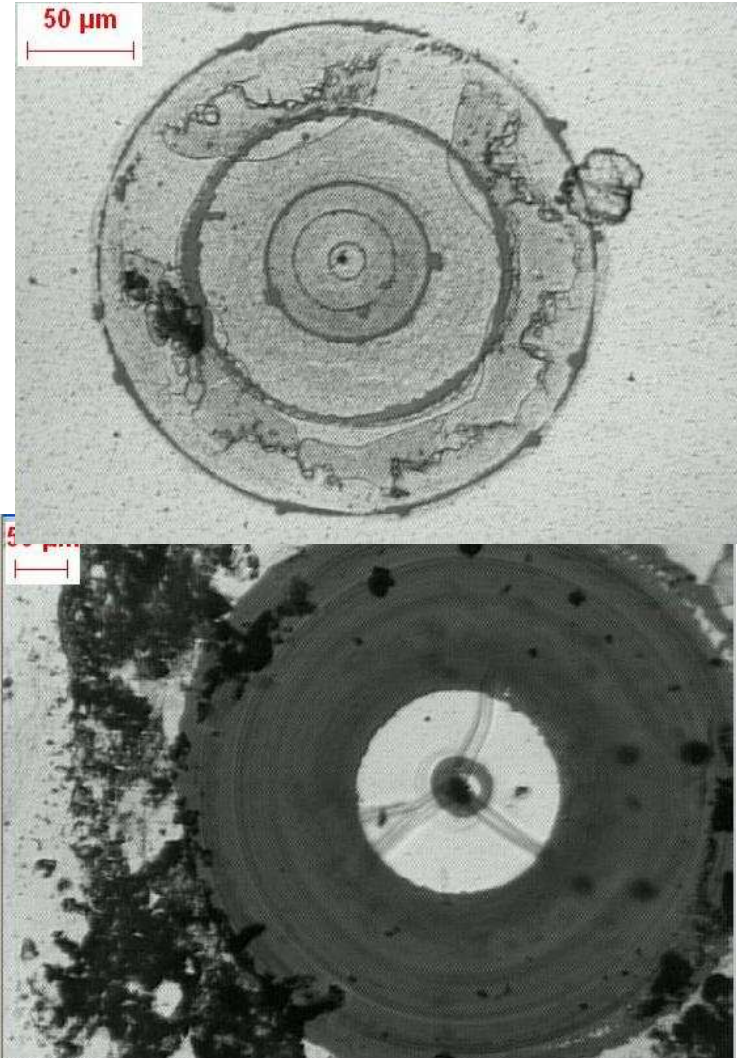


Force measurements can be used to detect defects in the dielectric.

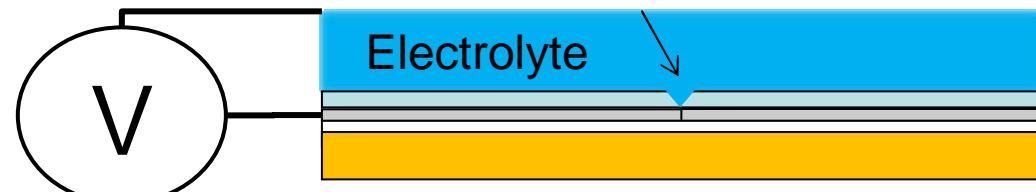
Nathan Crane, Vivek Ramadoss, USF



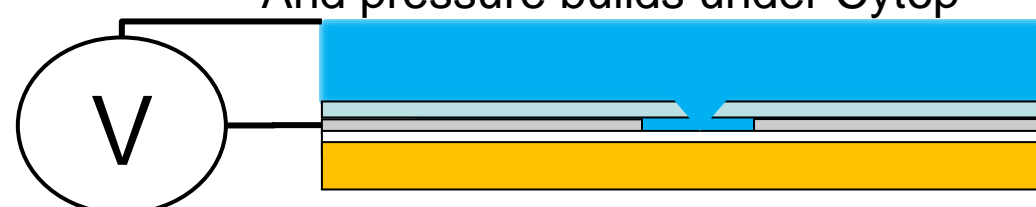
Possible Defect Mechanism



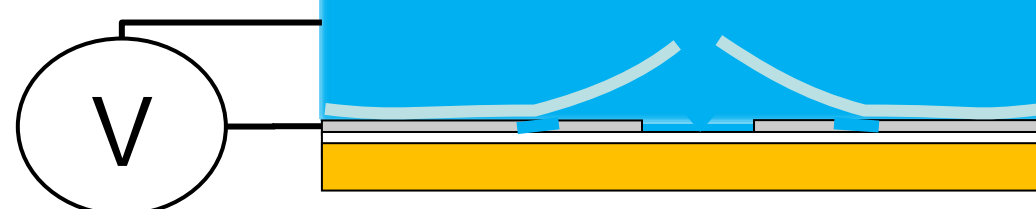
Hole forms in Cytop



Thin aluminum layer corrodes quickly
And pressure builds under Cytop



Cytop delaminates—exposing new Aluminum
Corrosion begins at Cytop/Aluminum Interface



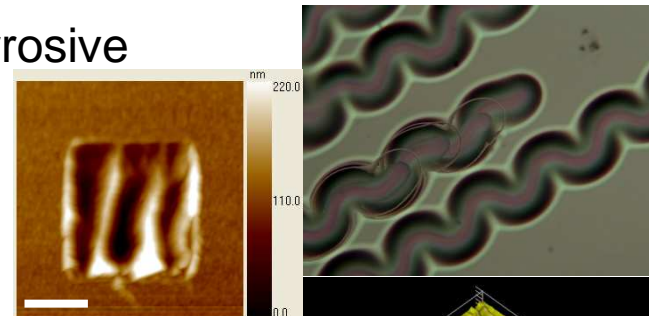
Conclusions for Electrowetting Experiments

- Electrowetting oscillation under a DC voltage input
- Proposed an explanation for this behavior based on local dielectric defects
- Introduced a method for measuring electrowetting forces in 2-axes simultaneously

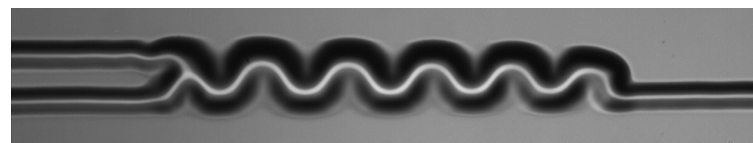
1. N.B. Crane, A.A. Volinsky, V. Ramadoss, M. Nellis, P. Mishra, X. Pang, MRS. Proc. Vol. 1052, DD8.1, 2008
2. N. Crane, A.A. Volinsky, P. Mishra, A. Rajgadkar, M. Khodayari, Appl. Phys. Lett., Vol. 96, pp. 104103-3, 2010
3. N. Crane, P. Mishra, A.A. Volinsky, Review of Scientific Instruments, Vol. 81, pp. 043902-7, 2010

Previously Funded Projects

NACE: "Adhesion Measurements of Thin Films in Corrosive Environments" \$40K



NSF: "Lab-on-a-chip Microchannels Novel Manufacturing Method" \$80K



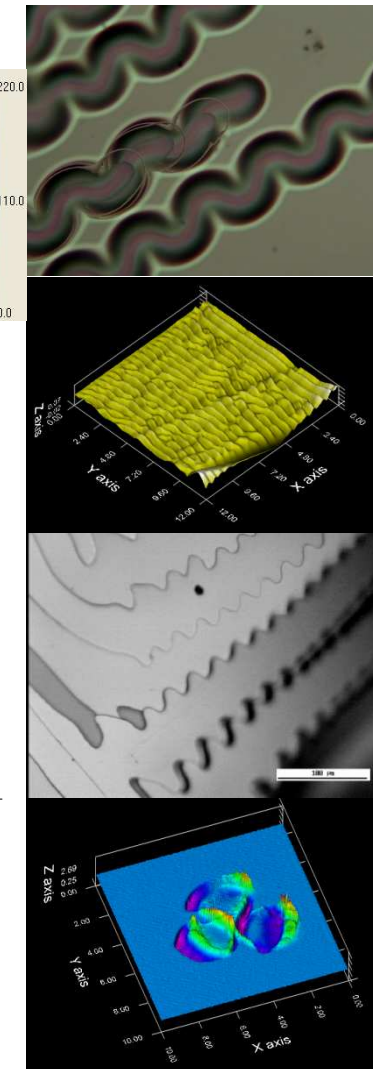
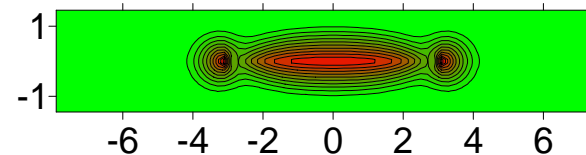
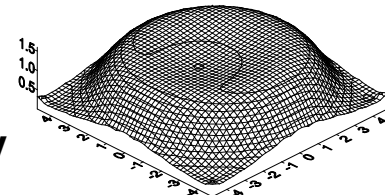
+IREE 2007 \$35K

Krakow, Poland

NSF: "Wear-induced Nanoripples in Single Crystals" \$60K

NSF: "Experimental and Computational Investigation of Fracture Patterns in Thin Films and Multilayers" \$250K

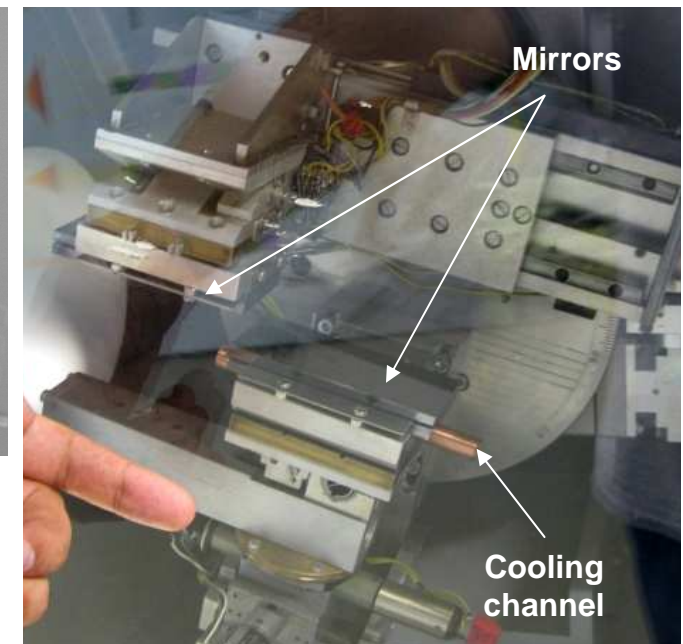
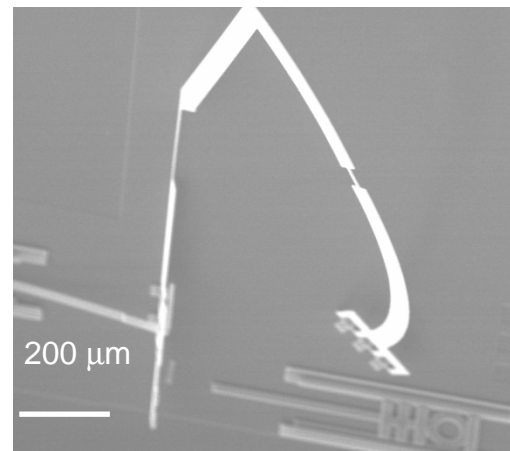
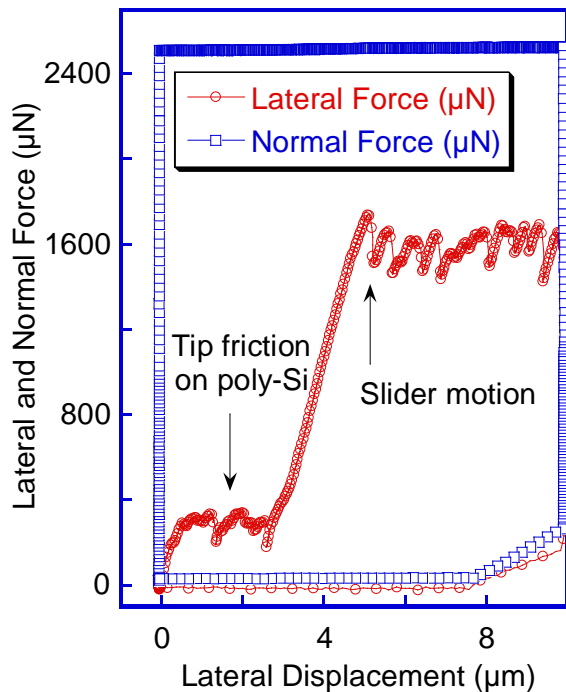
+IREE 2008 \$41K
Dresden, Germany



TI: "Nanoindentation and Modeling of Low-K Dielectrics for the TI Advanced Microelectronic Interconnects, their Mechanical Characterization and Reliability" \$15K

Currently Funded Projects

NSF: "Uncertainty Quantification for the Kinematic Approach to Compliant Mechanism Design" Co-PI with PI C. Lusk (USF) \$370K



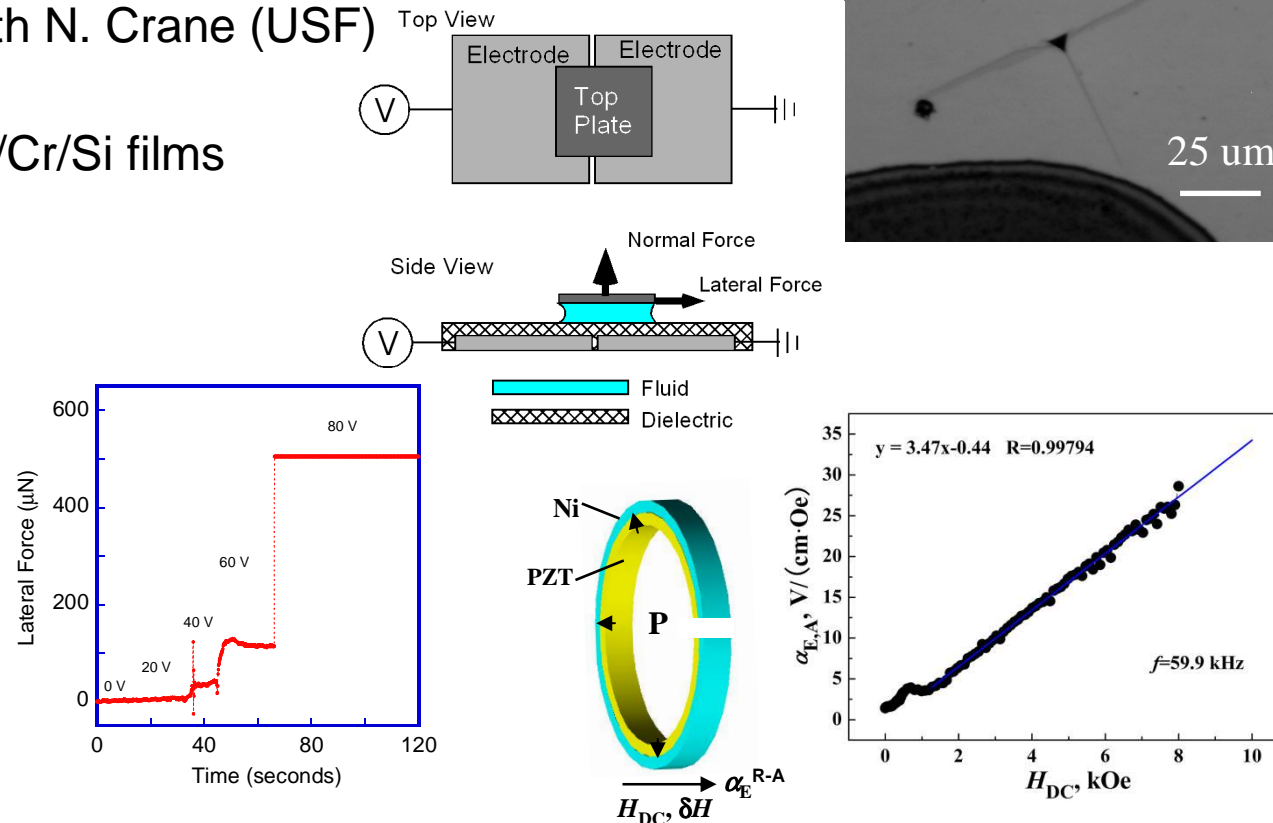
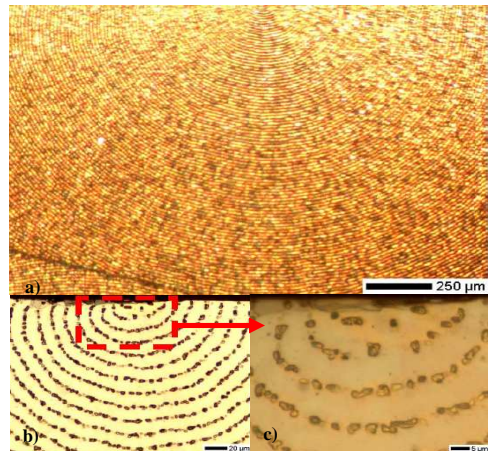
NSF: "IRES: International US-Germany Joint Study of X-Ray Optics Thermomechanical Stability and Control" \$150K.

Unfunded Projects

3C-SiC on Si mechanical properties with S. Saddow (USF)

Electrowetting forces with N. Crane (USF)

Pattern formation in Au/Cr/Si films
with D. Gracias (JHU)



Chromium oxide coatings on steel with Qiao, Gao and Pang,
Magnetolectric layered composites with D.A. Pan (USTB, China)

Summary

Hysitron TriboindenterTM and other equipment available at USF for collaborative research

We provide value added analysis.

